https://doi.org/10.5194/acp-2021-28
Preprint. Discussion started: 10 March 2021

Atmospheric Chemistry and Physics Discussions

Separating emission and meteorological contribution to $PM_{2.5}$ trends over East China during 2000–2018

Qingyang Xiao[1,#], Yixuan Zheng[2,#], Guannan Geng[1,3], Cuihong Chen[4,5], Xiaomeng Huang[4], Huizheng Che[6], Xiaoye Zhang[6], Kebin He[1,3], Qiang Zhang[4]

[1]State Key Joint Laboratory of Environment Simulation and Pollution Control, School of Environment, Tsinghua University, Beijing 100084, China
[2]Atmospheric Environment Institute, Chinese Academy of Environmental Planning, Beijing 100012, China
[3]State Environmental Protection Key Laboratory of Sources and Control of Air Pollution Complex, Beijing 100084, China
[4]Ministry of Education Key Laboratory for Earth System Modelling, Department of Earth System Science, Tsinghua University, Beijing 100084, China
[5]Satellite Environment Center, Ministry of Ecology and Environment of the People's Republic of China, Beijing 100094, China
[6]State Key Laboratory of Severe Weather & Key Laboratory of Atmospheric Chemistry of CMA, Chinese Academy of Meteorological Sciences, Beijing 100081, China

[#]These authors contributed equally to this work.

Correspondence to: Guannan Geng (guannangeng@tsinghua.edu.cn)

Abstract. The contribution of meteorology and emissions to long-term $PM_{2.5}$ trends is critical for air quality management but has not yet been fully analyzed. Here, we used a combination of machine learning model, statistical model and chemical transport model to quantify the meteorological impacts on $PM_{2.5}$ pollution during 2000–2018. Specifically, we first developed a two-stage machine learning $PM_{2.5}$ prediction model with a synthetic minority oversampling technique to improve the satellite-based $PM_{2.5}$ estimates over highly polluted days, thus allowing us to better characterize the meteorological effects on haze events. Then we used two methods, a generalized additive model (GAM) driven by the satellite-based full-coverage daily $PM_{2.5}$ retrievals as well as the Weather Research and Forecasting/Community Multiscale Air Quality (WRF/CMAQ) modelling system, to examine the meteorological contribution to $PM_{2.5}$. We found good agreements between the GAM model estimations and the CMAQ model estimations of meteorological contribution to $PM_{2.5}$ on monthly scale (correlation coefficient between 0.53–0.72). Both methods revealed the dominant role of emission changes in the long-term trend of $PM_{2.5}$ concentration in China during 2000–2018, with notable influence from the meteorological condition. The interannual trends in meteorology-associate $PM_{2.5}$ were dominated by the fall and winter meteorological conditions, when regional stagnant and stable conditions were more likely to happen and haze events frequently occurred. From 2000 to 2018, the meteorological contribution became more unfavorable to $PM_{2.5}$ pollution across the North China Plain and central China, but were more beneficial to pollution control across the southern part, e.g., the Yangtze River Delta. The meteorology-adjusted $PM_{2.5}$ over East China peaked at 2006 and 2011, mainly driven by the emission peaks in primary $PM_{2.5}$ and gas precursors in these years. Although emissions dominated the long-term $PM_{2.5}$ trends, the meteorology-driven anomalies also contributed –3.9% to 2.8% of the annual mean $PM_{2.5}$ concentrations in East China estimated from the GAM model. The meteorological contributions were even higher

https://doi.org/10.5194/acp-2021-28
Preprint. Discussion started: 10 March 2021


Atmospheric Chemistry and Physics Discussions

regionally, e.g., –6.3% to 4.9% of the annual mean $PM_{2.5}$ concentrations in the Beijing-Tianjin-Hebei region, –5.1% to 4.3% in the Fen-wei Plain, –4.8% to 4.3% in the Yangtze River Delta and –25.6% to 12.3% in the Pearl River Delta. Considering the remarkable meteorological effects on $PM_{2.5}$ and the worsening meteorological conditions in the northern part of China where air pollution was severe and population was clustered, stricter clean air actions are needed to avoid haze events in the future.

1 Introduction

The air pollution, especially $PM_{2.5}$ pollution, has become a serious problem in China in the past decades. Variations in air pollution are primarily driven by two factors: emissions and meteorology. Anthropogenic emissions dominate the long-term trend of air pollution (Zhang et al., 2019a;Cheng et al., 2019a), and meteorological conditions also notably influence the daily, seasonal, interannual and interdecadal air pollution variations (Zhang et al., 2018;Chen et al., 2020;Wang et al., 2019a;Zhai et al., 2019). In China, changes in major air pollutant emissions attributable to the economic development and clean air policies have been widely studied (Guan et al., 2014;Shen et al., 2017). For example, during the 11th Five-Year Plan (2006–2010) and the 12th Five-Year Plan (2011–2015), gas pollutant emissions, i.e., SO_2 and NO_x, have been remarkably reduced (Ma et al., 2019;Geng et al., 2019). During "the Air Pollution Prevention and Control Action Plan" (The Action Plan, 2013-2017) and the Blue Sky Protection Campaign (2018–2020), $PM_{2.5}$ emissions dropped significantly and the $PM_{2.5}$ concentrations substantially decreased (Bian et al., 2019;Liu et al., 2015). Meanwhile, air pollution was also affected by the long-term trend of meteorological systems and climate change, especially in the context of global warming (Ruijin et al., 2017;Wang and Chen, 2016;Yi et al., 2019;Zhang et al., 2019b). Distinguishing the contributions of emission and meteorology is critical for the evaluation of clean air policies, projection of the future air quality and understanding pollution process.

Various methods have been reported to separate the contributions of emissions and meteorology. For example, chemical transport models (CTMs) simulate the atmospheric process with emission inventory and meteorology fields as inputs, thus allowing researchers to assess the changes in air pollution attributable to one factor when controlling another factor (Wang et al., 2019a;Xu et al., 2020;Zheng et al., 2017). CTM simulations have been widely used to separate the contributions of meteorology and anthropogenic emissions to air pollution variations. With appropriate study design, the CTM modelling system can reasonably assess the influence of a specific emission reduction measure or a specific meteorological condition on air pollution. However, these model simulations require considerable computation resources, and the quality of inputs (e.g., emission inventory and meteorology) affects the quality of simulations. Moreover, due to the interactions between emissions and meteorology, the simulations in the fixed emission scenarios and the fixed meteorology scenarios may not fully reflect real-world conditions.

Other studies have applied statistical methods to assess the meteorology-associate changes in air pollution and to quantify the contribution of emissions. Multiple linear regression (MLR) has been adopted to describe the relationships between

https://doi.org/10.5194/acp-2021-28
Preprint. Discussion started: 10 March 2021


Atmospheric Chemistry and Physics Discussions

meteorology and air pollutant concentrations (Cheng et al., 2019a;Sá et al., 2015). For example, Zhai et al. (2019) constructed deseasonalized and deseasonalized-detrended time-series data and assessed the meteorological effects by MLR. Some studies also employed machine learning algorithms to better describe the non-linear relationships between meteorology and air pollution (Grange et al., 2018;Vu et al., 2019;Zhang et al., 2020). However, as such methods requires continuous $PM_{2.5}$ data as inputs, previous studies relied on $PM_{2.5}$ ground measurements that were limited to certain locations (e.g., ground monitoring stations) and times (e.g., after 2013 in China). The limited sample size not only affected the model quality and introducing sampling bias, but also hampered the analyses on spatial heterogeneity of meteorology contributions across China. The relatively short study period failed to show the long-term trend of meteorology-associate $PM_{2.5}$. The analysis on the complete-coverage long-term trends of meteorology and emission contributions to air pollution is urgently needed to support further evaluation of clean air policies and region-specific air quality management within the context of climate change.

In this study, we aimed to analyze the spatiotemporal trends in meteorology- and emission- associate $PM_{2.5}$ variations across China during 2000–2018. The meteorological impacts on $PM_{2.5}$ trends were assessed with data-fusion $PM_{2.5}$ predictions and chemical transport model simulations, taking advantage of the complete spatiotemporal coverage and long data records of these two datasets. The data-fusion $PM_{2.5}$ predictions were derived by combining satellite data, chemical transport model simulations, ground measurements and ancillary data with an optimized two-stage machine model that improved the $PM_{2.5}$ estimates during highly polluted days. Then we assessed the long-term variations in meteorology-associate $PM_{2.5}$ using a generalized additive model (GAM) that better described the non-linear associations between $PM_{2.5}$ and meteorology. We also estimated the meteorological impacts on $PM_{2.5}$ trends with chemical transport model simulations under different scenarios coupled with a most recent emission inventory. We showed that the temporal trends of meteorology-associate $PM_{2.5}$ estimated from the GAM method and from the chemical transport model were highly consistent. The trend analysis of the meteorology and emission contributions to $PM_{2.5}$ could support making of air quality management plans in the future.

2. Data and methods

This study employed simulations from the Weather Research and Forecasting/Community Multiscale Air Quality (WRF/CMAQ) modelling system as well as gridded $PM_{2.5}$ predictions fused from multiple data sources to assess the meteorological effects on $PM_{2.5}$ (Fig. 1). The study domain covers East China (east of longitude 105°) and the $PM_{2.5}$ concentrations during 2000–2018 were analyzed.

2.1 Satellite-based $PM_{2.5}$ retrievals

Previously reported satellite-based $PM_{2.5}$ data tended to underestimate high pollution events (Xiao et al., 2018;Xue et al., 2019) because these events rarely occurred in the model training dataset and were less characterized by the model. Since high pollution events were largely affected by meteorological conditions (Zhang et al., 2015;Liu et al., 2017b), correctly capturing

https://doi.org/10.5194/acp-2021-28
Preprint. Discussion started: 10 March 2021


Atmospheric Chemistry and Physics Discussions

these events was critical for the assessment of meteorological contributions. Thus, we developed a two-stage model to improve the prediction accuracy of $PM_{2.5}$ estimates, especially over highly polluted days, and obtained spatiotemporally continuous daily $PM_{2.5}$ dataset during 2000–2018.

2.1.1 Data for $PM_{2.5}$ modeling

We assimilated the daily $PM_{2.5}$ measurements, WRF/CMAQ simulations, satellite aerosol optical depth (AOD) from Aqua and Terra MODIS Level 2 products (https://ladsweb.modaps.eosdis.nasa.gov/), meteorological parameters from the Modern-Era Retrospective analysis for Research and Applications Version 2 (MERRA-2) (Randles et al., 2017;Buchard et al., 2017), elevation data from the Global Digital Elevation Model (GDEM) (https://earthexplorer.usgs.gov/), gridded population distributions (Xiao et al., 2021b), and land cover classification data (http://data.ess.tsinghua.edu.cn)(Gong et al., 2019a;Gong et al., 2019b) to train the $PM_{2.5}$ prediction model and predicted $PM_{2.5}$ concentrations during 2000–2018. The detailed data collection and processing methods were summarized in Appendix A.

2.1.2 The two-stage prediction model

A two-stage prediction model was developed to estimate $PM_{2.5}$ concentrations over China (Fig. 1). The first-stage model described high-pollution events that were underestimated in previous models, in which a synthetic minority oversampling technique (SMOTE) was adopted (Torgo, 2010). The second-stage model predicted $PM_{2.5}$ concentrations with the high-pollution indicator from the first-stage model.

Since high-pollution events relatively rarely occur in the model training dataset, the model may not appropriately characterize the associations between high $PM_{2.5}$ concentrations and the predictors, leading to underestimation of high-pollution levels (Wei et al., 2020). To balance high-pollution samples and normal samples, we first defined a high-pollution indicator, describing whether the daily $PM_{2.5}$ observation was higher than the monthly average $PM_{2.5}$ concentration plus two standard deviations at each location. A total of 3.9% of the daily data were assigned as high-pollution. Previous studies reported that balancing training data with SMOTE improved the classifiers' performance (Ghorbani and Ghousi, 2020;Saputra and Suharjito, 2019). Thus, we applied the SMOTE algorithm that oversampled the high-pollution data (the minority) by artificially generated new synthetic samples along the line between the high-pollution data and their selected nearest neighbors (Chawla et al., 2002;Chawla et al., 2003). This method also under-sampled the normal data (the majority) to better balance the uneven proportion of the high-pollution and normal data. With SMOTE resampling, high-pollution data accounted for 23% in the new model training dataset.

The balanced model training dataset was adopted to train the first-stage extreme gradient boosting (XGBoost) model with all the predictors, excluding CMAQ simulations. The predicted high-pollution indicator from the first-stage model was passed to the second-stage model as a predictor. We adopted the residual between the $PM_{2.5}$ measurement and the CMAQ $PM_{2.5}$

https://doi.org/10.5194/acp-2021-28
Preprint. Discussion started: 10 March 2021


Atmospheric Chemistry and Physics Discussions

simulation as the dependent variable to train the second-stage model. Training the model with residual enhances the response of predictors to $PM_{2.5}$ variations, thus improved the prediction accuracy.

To fill any missing satellite data, in both the first- and second-stage model, we assigned the availability of satellite retrievals as a dichotomous predictor and constructed it as the cutoff point of the first layer of the decision tree to separate the training data, thus mining the association between the availability of satellite retrievals and the $PM_{2.5}$ concentration. This method that fills missing $PM_{2.5}$ predictions with a decision tree outperformed other gap-filling methods in our previous evaluation study (Xiao et al., 2021a). The inclusion of CMAQ simulations also improved the accuracy of the gap-filled results.

The model's hyper parameter optimization and performance evaluation were conducted through five-fold CV, by-year CV and by-location CV (Appendix B).

2.2 Assessment of the meteorological effects on $PM_{2.5}$ using GAM

Following the method described by Zhai et al. (2019), we constructed time-series data to distinguish the long-term, seasonal, and short-term trends of $PM_{2.5}$ concentrations and meteorological conditions. Then the associations between $PM_{2.5}$ and meteorology were fitted with a GAM model, using daily satellite-based $PM_{2.5}$ predictions as dependent variable. GAM has been previously used to predict $PM_{2.5}$ concentrations with meteorology and other predictors (Yanosky et al., 2014;Liu et al., 2009;Xiao et al., 2018). The meteorological predictors in the GAM included 10-meter wind speed, 2-meter specific humidity, 2-meter air temperature, total precipitation, 10-meter eastward wind (U wind), 10-meter northward wind (V wind), U wind at 500 hpa, and planetary boundary layer height, which have been reported to be strongly associated with $PM_{2.5}$ concentrations in various regions in China (Chen et al., 2020).

Both the $PM_{2.5}$ data and the meteorology data followed the same processing protocol. First, we calculated 10-day average data, 50-day average data, and 19-year (2000–2018) average data based on the 50-day average data. We constructed deseasonalized-detrended data by removing the 50-day average data from the 10-day average data. We also constructed deseasonalized data by removing the 19-year average data from the 10-day average data. Assuming that the associations between $PM_{2.5}$ and meteorological parameters remained constant, we estimated these associations by a grid-specific seasonal and year-round GAM model (Pearce et al., 2011) with the deseasonalized-detrended data. The GAM allows a nonlinear response of $PM_{2.5}$ levels to meteorological conditions, thus providing better fits to the training data (Table B1). We also fitted grid-specific seasonal stepwise MLR in a sensitivity analysis to examine whether the selection of model affects the assessment of meteorological effects. Additionally, normalized meteorological parameters were used to fit the linear regression. Hence, the estimated coefficients reflected the relative contribution of each meteorological parameter and supported the spatial analysis of the meteorological effects. Since the seasonal model attained a higher average model R^2 than did the year-round model (Table B1), the results obtained with the seasonal model are presented in this study.

https://doi.org/10.5194/acp-2021-28
Preprint. Discussion started: 10 March 2021


Atmospheric Chemistry and Physics Discussions

2.3 Assessment of the meteorological effects on $PM_{2.5}$ using WRF/CMAQ

We also used the WRF/CMAQ model to separate the contribution of emissions and meteorology on $PM_{2.5}$ trends. The CMAQ model version 5.1 driven by the WRF model version v3.5.1 were utilized in this study, and the model configurations were following previous studies (Zheng et al., 2015, Zheng et al., 2017a). The initial and boundary conditions for WRF were derived from the National Centers for Environmental Prediction Final Analysis (NCEP-FNL) reanalysis data (NCEP, 2000). The boundary conditions for CMAQ were taken from the global GEOS-Chem model simulations. We used CB05 as the gas-phase mechanism, AERO6 as the aerosol module, and Regional Acid Deposition Model (RADM) as the aqueous-phase chemistry model in CMAQ. The anthropogenic emissions for mainland China were taken from the Multi-resolution Emission Inventory of China (MEIC(Maji et al., 2019)(Maji et al., 2019)(Maji et al., 2019)(Maji et al., 2019), http://meicmodel.org/)(Zheng et al., 2018;Li et al., 2017a), and emissions beyond mainland China were from the MIX Asian emission inventory (Li et al., 2017b).

Two scenarios were conducted to estimate the meteorological impacts on $PM_{2.5}$ trends, the *BASE* scenario and the *FixEmis* scenario. The *BASE* scenario was simulated with year-by-year emissions and meteorology during 2000–2018, while the *FixEmis* scenario was conducted using fixed emissions at the 2000 level and year-by-year meteorological inputs. The $PM_{2.5}$ simulations from the *BASE* scenario also supported the $PM_{2.5}$ estimates in Sect. 2.1.

The evaluation of meteorological simulations of surface temperature, surface relative humidity, surface wind speed, and surface wind direction from WRF against ground-level observations from the National Climate Data Center (NCDC, ftp://ftp.ncdc.noaa.gov/pub/data/noaa/) were summarized in Fig B1. The WRF model well repoduced the near-surface temperature (r=0.98, normalized mean bias=-1.9%) and relative humidity (r=0.81, normalized mean bias=5.4%), but slightly overestimated surface wind speed (r=0.57, normalized mean bias=8.0%). The WRF simulation quality of temperature, relative humidity and wind direction was consistent across years, but the simulation quality of wind speed showed slightly larger inter-annual variations. The validation results showed that the WRF simulations was acceptable to support further simulation of $PM_{2.5}$ concentrations. The evaluation of $PM_{2.5}$ simulations from CMAQ during the time period when ground measurements are available has been reported in our previous study (Zhang et al., 2019a). Compared to the measurements from ground monitoring stations, our model simulations well reproduced the spatial and temporal distributions of $PM_{2.5}$ across China. Compared to the daily $PM_{2.5}$ measurements in 74 cities, the CMAQ simulations obtained correlation coefficient r higher than 0.6 in 67 cities. The simulated $PM_{2.5}$ decrease (30%) during 2013-2017 over China also well matched the observed $PM_{2.5}$ decrease (33%).

3. Results and Discussion

3.1 Evaluation of the two-stage $PM_{2.5}$ prediction model

The SMOTE resampling approach improved the prediction accuracy in the five-fold CV that the area under the curve (AUC) increased from 90.7 to 98.7 (Fig. B2). The two-stage model predictions in the five-fold CV matched the ground measurements

https://doi.org/10.5194/acp-2021-28
Preprint. Discussion started: 10 March 2021


Atmospheric Chemistry and Physics Discussions

well with an R^2 of 0.80 and RMSE of 18.5 μg/m^3 (Fig. B2). The prediction accuracy in the by-location CV (R^2 of 0.71 and RMSE of 22.1 μg/m^3) and by-year CV (R^2 of 0.58 and RMSE of 27.5 μg/m^3) was lower than that in the five-fold CV, indicating unobserved temporal and spatial trends contributed to the $PM_{2.5}$ prediction. The model performance was comparable to that reported in previous studies (Xiao et al., 2018;He and Huang, 2018;Dong et al., 2020).

Specifically, compared to a benchmark model without SMOTE resampling and setting the $PM_{2.5}$ concentration as the dependent variable, the two-stage model in this study better predicted high-pollution events (Fig. 2). The density distribution of the $PM_{2.5}$ predictions from the two-stage model was very close to the density distribution of the $PM_{2.5}$ measurements. The density distribution of the $PM_{2.5}$ predictions from the benchmark model showed a higher percentage of low $PM_{2.5}$ concentrations and a lower percentage of high $PM_{2.5}$ concentrations than those revealed by the density distribution of the measurements. The greater ability of our two-stage model in capturing the daily variations in $PM_{2.5}$ concentrations could better support our following analysis about meteorological impacts.

3.2 Long-term trends of $PM_{2.5}$ concentrations over East China

Figure 3 shows the $PM_{2.5}$ trends during 2000–2018 in East China, as well as the key regions including the Beijing-Tianjin-Hebei (BTH) region, the Fen-wei Plain (FWP), the Yangtze River Delta (YRD) and the Pearl River Delta (PRD). The $PM_{2.5}$ concentrations continuously increased from 35.4 μg/m^3 in 2000 to 48.7 μg/m^3 in 2006 over East China. It then remained relatively constant from 2007–2013 and decreased from 46.5 μg/m^3 in 2013 to 32.5 μg/m^3 in 2018. BTH and FWP showed consistent temporal trends of $PM_{2.5}$, with higher pollution levels over BTH. However, the difference in $PM_{2.5}$ level between BTH and FWP has greatly decreased since 2015 due to the higher rate of $PM_{2.5}$ decrease in BTH resulting from the stricter emission control policies. The $PM_{2.5}$ level in the PRD reached its peak in 2006 and decreased thereafter. The observed $PM_{2.5}$ concentration in 2018 was 14.0, 30.9, 18.2, 22.9, and 13.2 μg/m^3 lower than that in 2013 over East China, BTH, FWP, YRD, and PRD, respectively.

3.3 Interannual and seasonal trends of meteorology-associate $PM_{2.5}$

Figure 4 shows the meteorological contribution in monthly average $PM_{2.5}$ concentrations estimated from the GAM model and CMAQ simulations. The temporal trends of meteorology-associate $PM_{2.5}$ estimated from these two methods were consistent across East China and in the key regions, with the correlation coefficients ranging between 0.53 (East China) and 0.72 (BTH). For example, the GAM model estimated typical favorable meteorological conditions in Oct 2013, Oct 2012 and Feb 2016 in BTH, which are also captured by the CMAQ model. However, the magnitude of the meteorological effects estimated by CMAQ were slight higher than GAM.

Figure 5 shows the GAM estimated temporal trend in meteorology-associate $PM_{2.5}$ across East China. Consistent with the CMAQ estimation (Fig. C1), 2012 is a typical year during which the meteorological conditions were favorable to $PM_{2.5}$ pollution control over East China, with an annual meteorology-associate $PM_{2.5}$ anomaly of -1.8 μg/m^3, 4.07%) (Fig. 5). 2004

https://doi.org/10.5194/acp-2021-28
Preprint. Discussion started: 10 March 2021


Atmospheric Chemistry and Physics Discussions

is a typical year during which the meteorological conditions were unfavorable to $PM_{2.5}$ pollution control, with an annual meteorology-associate $PM_{2.5}$ increase of 1.2 μg/m^3 (2.60%). The meteorological effects changed drastically over a relatively short time period. For example, in 2005, the meteorological conditions were greatly favorable to pollution control, but in the previous and following years, i.e., 2004 and 2006, respectively, the meteorological conditions were greatly unfavorable to pollution control. The long-term trend of the annual meteorology-associate $PM_{2.5}$ fluctuated about 0 across East China, with a decreasing trend (the meteorological conditions improving) from 2003–2010 and an increasing trend (the meteorological conditions worsening) from 2010–2017 (Fig. 5, Fig. B3). The CMAQ simulations estimated the largest unfavourable meteorological contribution in 2018 of 11.0%, and the greatest benefical meteorological contribution in 2012 of 7.2% over East China.

The interannual variations in the meteorology-associate $PM_{2.5}$ assessed in this study were consistent with those reported in previous studies (Zhang et al., 2018). For example, Feng et al. (2020) presented the long-term variations in air stagnation in north China that characterized the circulation and diffusion in the boundary layer with fixed emissions to describe the temporal trend of haze-related weather conditions. The temporal pattern of the air stagnation index from 2000–2018 was closely resembled the temporal trend of the estimated meteorological-associate $PM_{2.5}$ in this study. Additionally, we observed unfavorable meteorological conditions in the winters of 2014 and 2016, consistent with the previously reported climate anomalies in these two years (Yin et al., 2017;Yin and Wang, 2017). We also showed that the meteorological conditions in 2014 and 2015 were more unfavorable to $PM_{2.5}$ pollution control than those in 2013 over East China, as previously reported (Zhang et al., 2019b;Wang et al., 2019a).

Since haze events that greatly affects public health mainly occur in fall and winter (Zhao et al., 2013), we further analyzed the meteorological effects during fall-winter (September, October, November, December, January, and February) and spring-summer. The meteorological conditions in fall-winter dominated the annual meteorological effects on $PM_{2.5}$. We observed typical unfavorable meteorological conditions in the fall-winter of year 2006 (2.8 μg/m^3) and 2016 (2.5 μg/m^3). In certain years, e.g., 2018, the spring-summer meteorological conditions were unfavorable to pollution control, but since the fall-winter meteorological conditions were favorable, the annual meteorological effect was beneficial. The significant fall-winter meteorological effects indicated the critical contribution of meteorology to haze event formation. The fall-winter weather conditions in 2017 were substantially better than the fall-winter weather conditions in 2013, leading to a 3.3 μg/m^3 decrease in the meteorology-associate $PM_{2.5}$, thereby contributed to the achievement of pollution control targets of the Action Plan (Zhang et al., 2019b;Yi et al., 2019). Since the current evaluation of clean air policies focuses on changes in pollution levels over short periods, e.g., three or five years, policy performance can be largely affected by meteorological changes.

3.4 Spatial heterogeneity in meteorology-associate $PM_{2.5}$ trends

We also analyzed the variations in the meteorological influence on $PM_{2.5}$ in several populous urban agglomeration regions of China (Fig. 5, Fig. B3). In the BTH region, 2014 was a typically unfavorable year (3.1 μg/m^3), and 2010 was a typically

https://doi.org/10.5194/acp-2021-28
Preprint. Discussion started: 10 March 2021


Atmospheric Chemistry and Physics Discussions

favorable year (-4.9 μg/m^3). The shape of the interannual trend of the meteorology-associate $PM_{2.5}$ during wintertime in BTH was consistent with that in previous studies. For example, the 2014 and 2017 winter meteorological conditions were greatly favourable and the 2016 winter meteorological conditions were considerably unfavorable (Yi et al., 2019;Wang and Zhang, 2020). The meteorological effects showed a regional consistency with varying magnitudes. For example, 2004 was a typical unfavorable year in both the PRD (6.3 μg/m^3) and the YRD (2.7 μg/m^3), and 2016 was a typical favorable year in both the PRD (-7.3 μg/m^3) and the YRD (-2.1 μg/m^3). Consistent with previous studies, the PRD revealed the largest meteorological influence on $PM_{2.5}$ among these regions (Zhai et al., 2019).

We observed notable regional heterogeneity in the long-term trends as well as seasonal trends of the meteorological effects on $PM_{2.5}$ (Fig. 5, Fig. B3). In the northern part of China, especially in the North China Plain and central East China, the meteorological conditions worsened and were adverse to pollution control (Yin and Wang, 2018;Zhang et al., 2018). Multiple climate systems could be associated with the long-term trend of meteorological effects. For example, greenhouse gas-induced warming may result in a decrease in light-precipitation days and surface wind speed, which are unfavorable to pollution control (Chen et al., 2019). In contrast, in the southern part of China, especially in the YRD and surrounding regions, the estimated meteorological conditions were improving and were beneficial to pollution control (Chen et al., 2019).

Regarding the seasonal trend of the meteorological effects, in spring-summer, we observed improving meteorological effects in the southern part of China and worsening meteorological effects in the northern part of China. This spatially heterogeneous trend may result from the strengthening of the East Asia summer monsoon, which enhances the transportation of aerosols from the south to the north of China (Zhu et al., 2012;Liu et al., 2017a). In fall-winter, the East Asia winter monsoon significantly affects air pollution levels that benefits the air quality in North China but is unfavourable to air quality in the South China due to the southward transport of pollutant from north to south (Jeong and Park, 2017;Yin et al., 2015). For example, in the year 2004, 2005, 2007, and 2010 with strong East Asia winter monsoon, the BTH and the FWP showed strong favourable meteorology contributions to $PM_{2.5}$, but the YRD and the PRD showed unfavourable meteorological effects. On the contrary, in the year 2006 with weak East Asia winter monsoon, the BTH and the FWP showed unfavourable meteorological effects (Jeong and Park, 2017).

The large-scale atmospheric circulations in some specific years also showed notably distinct effects on $PM_{2.5}$ concentrations over the north and south of East China, due to the opposite effects on meteorology parameters. For example, in 2015 and 2016 with strong El Niño, the fall-winter meteorology in the northern part of East China was significantly unfavorable for pollution control but that in the southern part of East China was considerably favorable. One reason is that the El Niño leads to excessive precipitation over southern China that in favour of wet deposition, but weakened the East Asia winter monsoon and led to south wind anomaly, weaker surface wind, and high humidity that were favorable to pollution events in the northern region of East China (Yin et al., 2015;Yin and Wang, 2016;He et al., 2019;Chang et al., 2016). On the country, during the year with La Niña , e.g. 2007 and 2010, we estimated beneficial winter-fall meteorology in northern regions but unfavourable meteorology in the southern region (Cheng et al., 2019b).

https://doi.org/10.5194/acp-2021-28
Preprint. Discussion started: 10 March 2021


Atmospheric Chemistry and Physics Discussions

Consistent with previous studies, we also observed spatially varying associations between $PM_{2.5}$ and meteorological parameters that reflect the varying $PM_{2.5}$ responses to meteorological changes (Fig. B4). Temperature was positively associated with $PM_{2.5}$ in spring, summer and fall across East China; however, in winter, the temperature was negatively associated with $PM_{2.5}$ in northern China (He and Wang, 2017;Qiu et al., 2015) due to the low-temperature-related stable atmosphere and decreased evaporation loss of $PM_{2.5}$. Humidity yielded positive effects in northern China and negative effects in southern China in all seasons, especially in winter (He et al., 2017). The spatial difference in the effects of humidity on $PM_{2.5}$ may occur due to a threshold of the humidity altering the direction of the humidity influence, from hygroscopic increase to wet deposition. The boundary height and precipitation were negatively associated with $PM_{2.5}$ across East China in all seasons, and the effect of precipitation was greater in northern China than that in southern China (Wang and Chen, 2016). Regarding the relative contribution of the different meteorology parameters, we found that over the south coast region, temperature and humidity showed greater effects than did the boundary layer height and precipitation. In winter, humidity, boundary layer height and precipitation were critical for the $PM_{2.5}$ variations in the middle and north of China. In summer and fall, the temperature and humidity were critical for the $PM_{2.5}$ variations across southern China. In spring, the temperature showed notable effects in the south coast region, and the precipitation exhibited large effects in the North China Plain.

3.5 $PM_{2.5}$ trends after adjusting the meteorological effects

In East China, after adjusting for the meteorological influence, $PM_{2.5}$ started increasing in 2000 and peaked in 2006 with an increase of 9.6 $\mu g/m^3$ compared to the 2000 level (Fig. 6). Then, the $PM_{2.5}$ varied, with the second highest $PM_{2.5}$ level occurring in 2011 (9.4 $\mu g/m^3$ higher than the 2000 level). After 2013, with the implementation of aggressive emission control policies, $PM_{2.5}$ notably decreased, with a 13.1 $\mu g/m^3$ lower $PM_{2.5}$ level in 2018 compared to the level in 2013. After adjusting for the meteorological effects, the temporal variations in $PM_{2.5}$ were consistent with the temporal variations in pollutant emissions retrieved from the MEIC emissions. The emissions of SO_2 and $PM_{2.5}$ peaked in 2006, and the emissions of NO_x peaked in 2012.

In the BTH region, $PM_{2.5}$ peaked in 2006 and decreased by 10.8 $\mu g/m^3$ in 2008 due to the emission control policies targeting the air quality during 2008 Beijing Olympic Games. After 2008, $PM_{2.5}$ continuously increased and peaked in 2013, at an increase rate of 1.0 $\mu g/m^3$ per year. Considering the variations in pollutant emissions, the first $PM_{2.5}$ peak in BTH was primarily driven by SO_2 emissions, and the second $PM_{2.5}$ peak was driven by NO_2 and $PM_{2.5}$ emissions. The $PM_{2.5}$ decreasing trend after 2013 in BTH was higher than that in the other regions (5.8 $\mu g/m^3$ per year), mainly driven by the emission reduction in SO_2 and $PM_{2.5}$. The annual average meteorology-adjusted $PM_{2.5}$ concentration in BTH from 2014-2018 was consistent with that in a previous study (Qu et al., 2020). We found that the observed high-pollution events in the fall-winter of year 2006, 2013, and 2016 were partly attributable to unfavorable meteorological conditions that led to a 5.9, 3.4, and 11.1 $\mu g/m^3$ $PM_{2.5}$ increase, respectively. Since the meteorology contributed up to 25% of the observed $PM_{2.5}$ level in fall-winter, further emission control measures are needed to improve the winter air quality and avoid violations of the air

https://doi.org/10.5194/acp-2021-28
Preprint. Discussion started: 10 March 2021


Atmospheric Chemistry and Physics Discussions

quality standards under unfavorable meteorological conditions. In FWP, the highest $PM_{2.5}$ level occurred in 2005, and the average decrease rate after 2013 was 2.8 μg/m^3 per year. The high pollution in the 2016 fall-winter period attributable to unfavorable meteorological conditions was also observed in FWP, although the meteorological effects in FWP were smaller than those in the BTH region, with up to 10% of the meteorology contribution in $PM_{2.5}$ in fall-winter. In the YRD, $PM_{2.5}$ peaked in 2011 and 2015. The unfavorable meteorological conditions observed in the fall-winter of 2016 did not occur in either the YRD or the PRD, showing a spatial difference in the meteorological system. In the PRD, $PM_{2.5}$ peaked in 2006 and continuously decreased from 2006-2018, at an average decrease rate of 2.8 μg/m^3 per year. This decreasing trend was consistent with the trend of the $PM_{2.5}$ emissions. The temporal variations in NO_x and SO_2 emissions contributed to the trends in the meteorology-adjusted $PM_{2.5}$ from 2010–2011.

It is observed that although emissions dominated the interannual variations in $PM_{2.5}$, meteorological conditions significantly affected the observed $PM_{2.5}$ concentration in all key regions, especially in fall and winter. We observed as much as 25.6%, 6.3%, 5.1% and 4.8% annual average meteorological effects, estimated from GAM, in the PRD, BTH, FWP, and YRD, respectively, during the study period. The meteorological contributions in fall-winter were even higher. The CMAQ simulations estimated as much as 17.5%, 8.8%, 26.6%, and 6.6% annual average meteorological effects in the PRD, BTH, FWP, and YRD, respectively. From 2015 to 2016, the winter-fall meteorological conditions considerably changed to unfavorable for pollution control in North China, leading to a 2.8 μg/m^3 increase in the winter-fall average $PM_{2.5}$ concentration across East China. BTH and FWP showed a 9.8 and 8.1 μg/m^3 increase, respectively. Such an increase may weaken the effects of emission control policies during this period. In 2018, the $PM_{2.5}$ concentration in Beijing was reported to be 51 μg/m^3. However, if 2018 had been a typical year with unfavorable meteorological conditions, the annual $PM_{2.5}$ concentration could have reached 54 μg/m^3.

The meteorology-adjusted $PM_{2.5}$ trend from 2013-2018 showed varying spatial patterns. The highest decrease occurred in Beijing, Tianjin, south of Hebei and the capital cities, including Xi'an, Wuhan, Zhengzhou, and Changsha (Fig. 7), indicating the more efficient implementation of clean air policies in these regions. As described above, the effects of meteorology also showed spatial differences. Over the Northeast China Plain, North China Plain, and Sichuan Basin, the adjusted $PM_{2.5}$ decreasing trend was weaker than the observed trend. Over the Shanxi, the intersection of Hubei-Henan-Anhui and south of Jiangsu, the adjusted $PM_{2.5}$ decreasing trend was stronger than the observed trend. The interquartile range of the meteorological effects on the $PM_{2.5}$ trend varied between -17.2% and 1.8% across East China. From 2013-2018, the decreasing trend of the meteorology-adjusted $PM_{2.5}$ level was lower than that of the observed $PM_{2.5}$ level by 8.4% in East China, 7.9% in the BTH region, 3.3% in the YRD, and 7.5% in the PRD while the adjusted trend was greater than the observed trend by 2.01% in the FWP.

https://doi.org/10.5194/acp-2021-28
Preprint. Discussion started: 10 March 2021


Atmospheric Chemistry and Physics Discussions

3.6 Sensitivity analysis

To evaluate whether the selection of statistical models affects the assessed associations between meteorology and $PM_{2.5}$, we compared the meteorology-associate $PM_{2.5}$ estimated by GAM and MLR. The estimated meteorology-associate $PM_{2.5}$ levels from the MLR and GAM matched well, with correlation coefficients larger than 0.98 across East China (Fig. B5). Hence, the results of this study are robust and not affected by the selection of $PM_{2.5}$-meteorology model.

To examine the effects of length of the time window when constructing the deseasonalized $PM_{2.5}$, we conducted a sensitivity analysis with a 90-day averaging window in the BTH region, and the estimated $PM_{2.5}$ concentrations after adjusting for meteorological effects were almost identical to the results using a 50-day time window (Fig. B5). Thus, this statistical method was not sensitive to the averaging time window.

Compared to previous studies, we employed the GAM to better describe the nonlinear associations between $PM_{2.5}$ and meteorology in this study. We observed consistent temporal trends of the meteorological effects and the meteorologically adjusted $PM_{2.5}$ concentrations compared to previous studies, but the magnitude of the assessed meteorological effects and adjusted $PM_{2.5}$ concentrations varied. Thus, when comparing the meteorological effects of a specific year, the conclusion may be inconsistent (Xu et al., 2020;Zhai et al., 2019;Zhang et al., 2019a;Zhang et al., 2019b). Assessing the meteorology-associate $PM_{2.5}$ with different methods may also lead to varying long-term trends (Xu et al., 2020). Several factors may affect the uncertainty of the assessed meteorological contributions in this study. First, the satellite retrievals exhibited an increasing prediction error when hindcasting historical pollution levels. The satellite-driven $PM_{2.5}$ prediction model used in this study is a state-of-the-art prediction model with improved prediction accuracy for high-pollution events, but the hindcast prediction quality needs to be further improved to better describe the historical $PM_{2.5}$ spatiotemporal distribution. Second, we obtained meteorological information from the MERRA-2 reanalysis dataset with a spatial resolution lower than that of the $PM_{2.5}$ predictions. This resolution mismatch with smooth spatial variations in the meteorological fields may not fully describe the meteorological effects at the local scale.

4. Conclusions

In this study, we analyzed the meteorology- and emission-driven variations in the $PM_{2.5}$ concentration during 2000-2018 across East China by the GAM-based method and CMAQ simulations. To support the GAM-based analysis, we combined satellite data, CMAQ simulations and ground observations to predict complete-coverage $PM_{2.5}$ concentrations with a two-stage machine learning model that attained improved prediction accuracy of high-pollution events. Both methods showed significant meteorological influences on $PM_{2.5}$ dominated by the meteorological conditions in fall and winter. The greatly varying meteorological effects on $PM_{2.5}$ concentration over a relatively short time period may remarkably affect the evaluation of clean air policies during a certain period. We also observed distinct regional differences in the long-term and seasonal trends of the meteorological effects. The meteorology-associate $PM_{2.5}$ tended to increase in the North China Plain and Central China, but

https://doi.org/10.5194/acp-2021-28
Preprint. Discussion started: 10 March 2021


Atmospheric Chemistry and Physics Discussions

decrease across southern China, e.g. in the YRD. After adjusting for the meteorological effects, the average $PM_{2.5}$ concentration decreased 13.1 μg/m^3 from 2013–2018 over East China, and the BTH region showed the greatest decrease (28.5 μg/m^3) among the studied urban agglomeration regions. The decreasing trend of $PM_{2.5}$ after adjusting for the meteorological effects was 8.4% weak than the observed $PM_{2.5}$ decreasing trend in East China, 7.9% weak in the BTH region, 3.3% weak in the YRD, and 7.5% weak in the PRD while the adjusted trend was 2.0% greater than the observed trend in the FWP. Considering the remarkable meteorological contributions to $PM_{2.5}$, further emission reduction measures are required to prevent the occurrence of haze events under unfavourable meteorological conditions.

Appendix A. Data collection and processing

We collected hourly $PM_{2.5}$ measurements from 2013-2018 from both the national air quality monitoring network (~1,593 stations) and local air quality monitoring stations (~ 1,700 stations) mainly located in East China. Continuous identical measurements over at least three hours were removed due to instrument malfunction. Daily average concentrations were calculated based on at least 12 hourly measurements.

We obtained Aqua and Terra MODIS Collection 6 level 2 aerosol products at a 0.1-degree resolution from https://ladsweb.modaps.eosdis.nasa.gov/. Since the aerosol optical depth (AOD) retrieved with the Deep Blue (DB) algorithm and the Dart Target (DT) algorithm (Levy et al., 2013;Hsu et al., 2013) exhibit different coverage and retrieval accuracy (Wang et al., 2019b), we fitted daily linear regressions to fill the missing retrievals when only DT or DB AOD was presented. Then, we calculated the average of the DT AOD and DB AOD separately for each sensor. Similarly, since the Aqua AOD and Terra AOD are observed at different pass over times, to improve the data coverage, we fitted daily linear regressions to fill the missing retrievals when only Aqua AOD or Terra AOD was presented. We calculated the average of the Aqua and Terra AODs to characterize the daily aerosol loadings (Jinnagara Puttaswamy et al., 2014).

We also used daily $PM_{2.5}$ simulations at a spatial resolution of 36 km during 2000-2018 from the WRF/CMAQ model as an important predictor. The inverse distance weighting (IDW) method was applied to interpolate the CMAQ simulations to match the grid of 0.1°. Detailed description of the WRF/CMAQ simulations could be found in Sect. 2.3.

Meteorological parameters were extracted from the Modern-Era Retrospective analysis for Research and Applications Version 2 (MERRA-2) dataset at a resolution of 0.5° latitude × 0.625° longitude (Randles et al., 2017). We extracted parameters including surface albedo, cloud area fraction for low clouds, total cloud area fraction, surface net downward longwave flux, surface incoming shortwave flux, surface net downward shortwave flux, total incoming shortwave flux, total net downward shortwave flux, surface pressure, 2-meter specific humidity, 2-meter air temperature, 2-m dew point temperature, total column ozone, total column odd oxygen, total precipitable ice water, total precipitable liquid water, total precipitable water vapor, 2-meter eastward wind (U wind), 2-meter northward wind (V wind), 10-meter U wind, 10-meter wind speed, 10-meter V wind, U wind at 500 hPa, U wind at 850 hPa, V wind at 500 hPa, V wind at 850 hPa, total latent

https://doi.org/10.5194/acp-2021-28
Preprint. Discussion started: 10 March 2021


Atmospheric Chemistry and Physics Discussions

energy flux, evaporation from turbulence, planetary boundary layer height, snowfall, and bias-corrected total precipitation. These parameters have been reported to be strongly associated with the $PM_{2.5}$ concentration in various regions in China (Chen et al., 2020). The inverse distance weighting method was applied to estimate the daily smooth surface of meteorological data and to match with the modelling grid at a 0.1° spatial resolution.

Elevation data from the Global Digital Elevation Model (GDEM, https://earthexplorer.usgs.gov/) version 2 at a 30-m resolution were averaged to match the modelling grid. We calibrated the gridded population distribution data from the LandScan Global Population Database (https://landscan.ornl.gov/), the Gridded Population of the World (GPW, https://beta.sedac.ciesin.columbia.edu/data/set/gpw-v4-population-count) dataset and the WorldPop dataset (https://www.worldpop.org/) at the county level with the total population reported in China City Yearbooks. These calibrated gridded population data were fused to better characterize the population distribution across China (Xiao et al., 2020).The land cover classification data of urban and rural regions at a 30-m resolution for 2000-2017 were downloaded from http://data.ess.tsinghua.edu.cn (Gong et al., 2019a;Gong et al., 2019b). The fraction of urban/rural region at the 30-m resolution was averaged according to the modelling grid.

https://doi.org/10.5194/acp-2021-28
Preprint. Discussion started: 10 March 2021


Atmospheric Chemistry and Physics Discussions

Appendix B. Model performance evaluation

The hyperparameters of XGBoost, including the maximum number of boosting iterations, the learning rate, the maximum depth of a tree, the minimum sum of the instance weight needed in a child, the subsampling ratio of a training instance, and the subsampling ratio of columns when constructing each tree, were optimized by grid search with the five-fold cross-validation (CV) root-mean-square error (RMSE) as a performance evaluation statistic.

The model performance was evaluated through five-fold CV, by-year CV and by-location CV. The five-fold CV approach randomly selects 20% of the data for model testing and train the model with the remaining data. This process is repeated five times, and each record is selected once as testing data. The by-year CV approach validates the model hindcast ability by sequentially selecting one year of data for testing and using the remaining yearly data for model training such that each year is selected once for testing. The by-location CV approach validates the model ability for spatial prediction by using the data at 20% randomly selected locations for testing and uses the remaining data for model training. This process is repeated five times until each location has been selected once for model testing.

https://doi.org/10.5194/acp-2021-28
Preprint. Discussion started: 10 March 2021

Atmospheric Chemistry and Physics Discussions

435

Table B1. Model fitting average R^2 value of the seasonal generalized additive model (GAM), year-round GAM, seasonal stepwise multiple linear regression (MLR), and year-round MLR.

	Spring	Summer	Fall	Winter	Year-round
Seasonal GAM	0.39	0.45	0.42	0.48	
Year-round GAM					0.32
Seasonal MLR	0.34	0.40	0.37	0.42	
Year-round MLR					0.26

https://doi.org/10.5194/acp-2021-28
Preprint. Discussion started: 10 March 2021

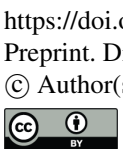

Atmospheric Chemistry and Physics Discussions

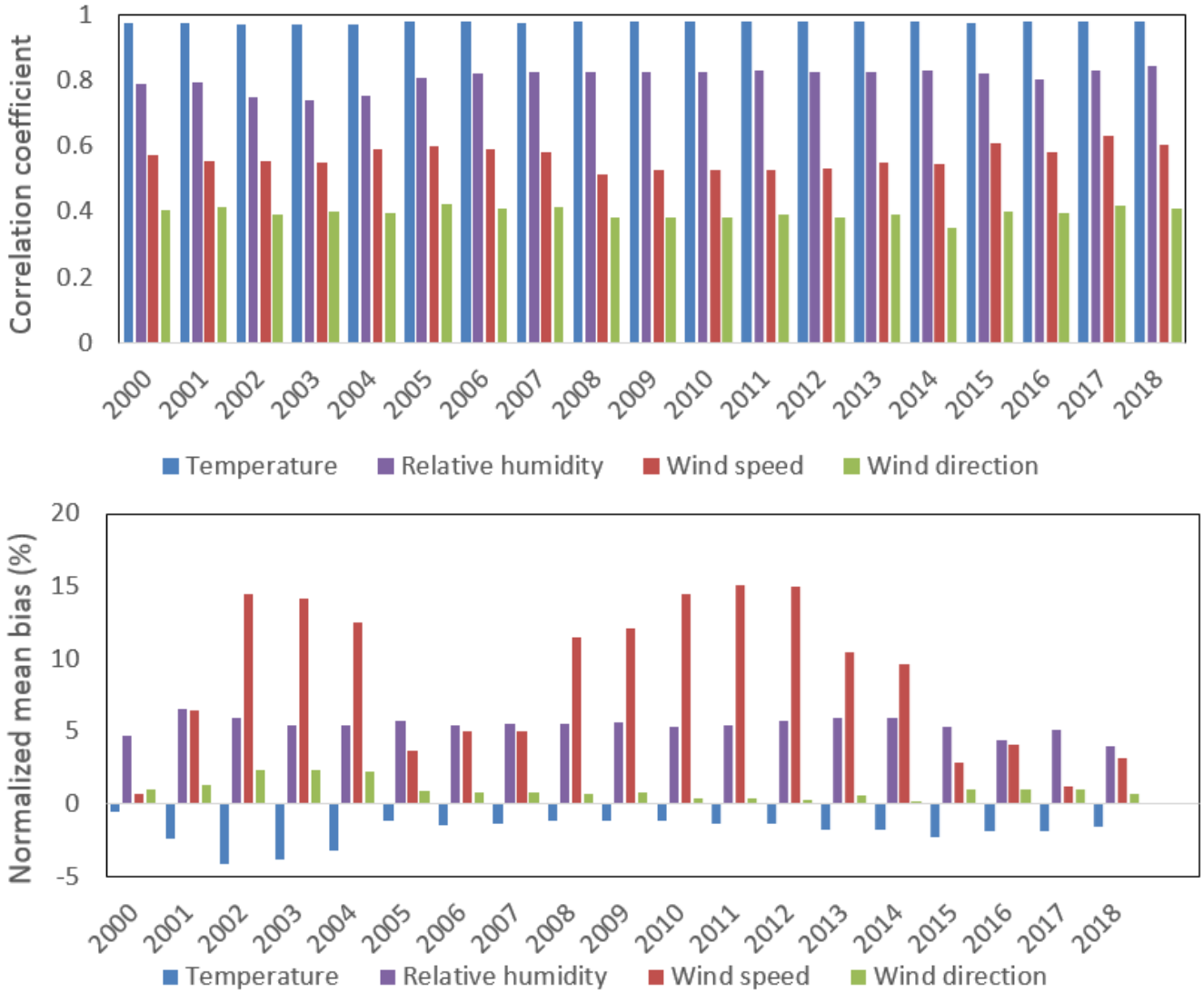

Figure B1: Evaluation of the WRF model simulations. The correlation coefficient and normalized mean bias was calculated by comparing WRF simulations with ground observations from the National Climate Data Center.

https://doi.org/10.5194/acp-2021-28
Preprint. Discussion started: 10 March 2021

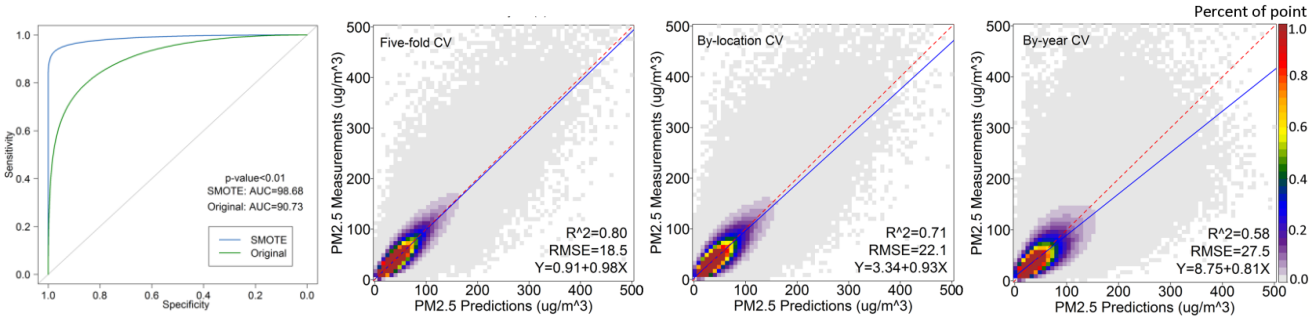

Figure B2: Model evaluation of the first-stage model trained with the original dataset and the SMOTE-resampled dataset in five-fold cross-validation (CV) and scatter plots comparing the ground measurements and model predictions in five-fold CV, by-location CV and by-year CV.

https://doi.org/10.5194/acp-2021-28
Preprint. Discussion started: 10 March 2021

Atmospheric Chemistry and Physics Discussions

Appendix C. Meteorological contributions to $PM_{2.5}$.

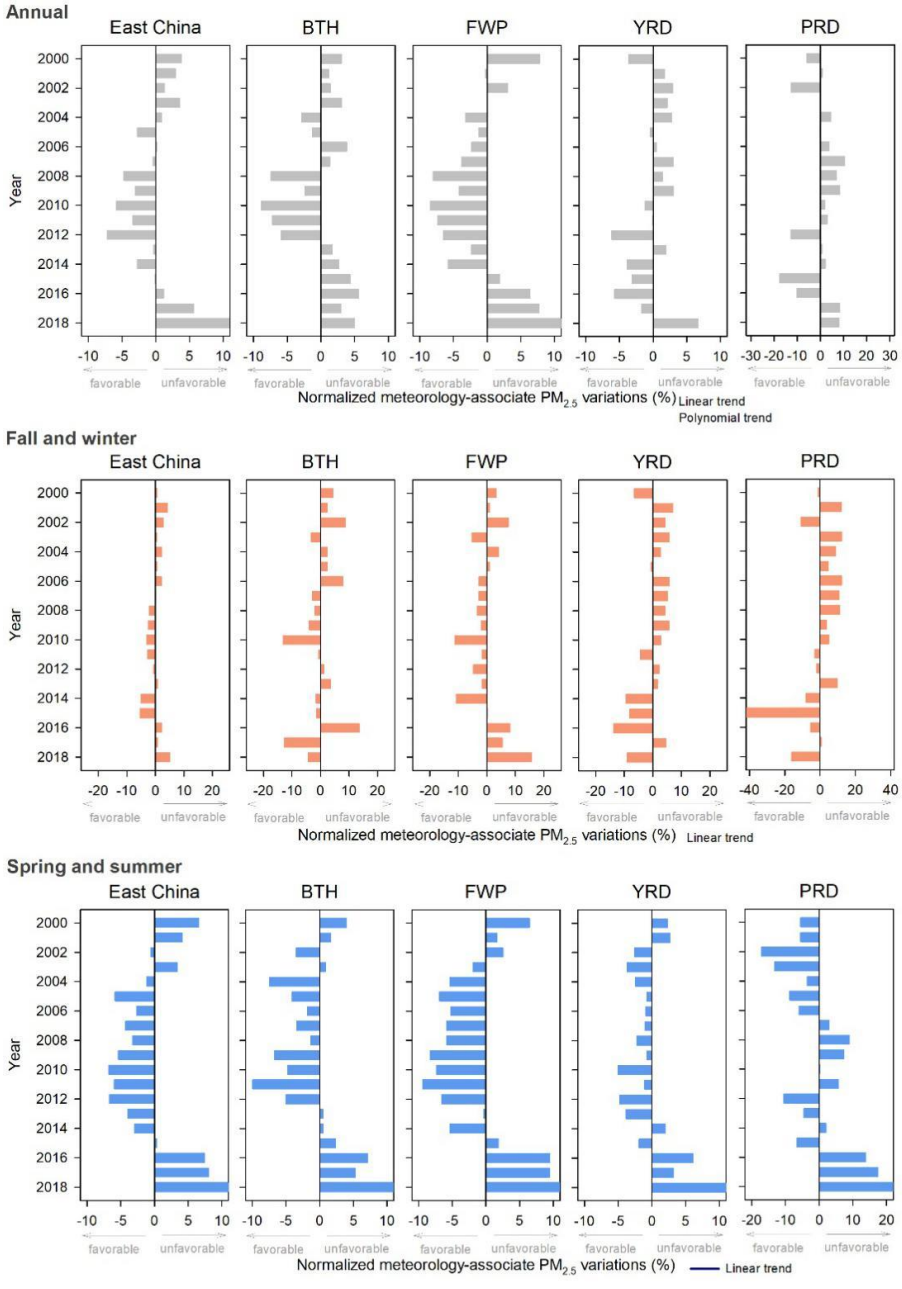

Figure C1: The CMAQ estimated relative impact of meteorology on annual average $PM_{2.5}$ (top row), relative impact of meteorology on average $PM_{2.5}$ in fall-winter (September, October, November, December, January in next year, and February in next year) (middle), and relative impact of meteorology on average $PM_{2.5}$ in spring-summer (bottom row) with the long-term trends estimated by polynomial and linear regression over East China, BTH, FWP, YRD, and PRD.

https://doi.org/10.5194/acp-2021-28
Preprint. Discussion started: 10 March 2021

Atmospheric Chemistry and Physics Discussions

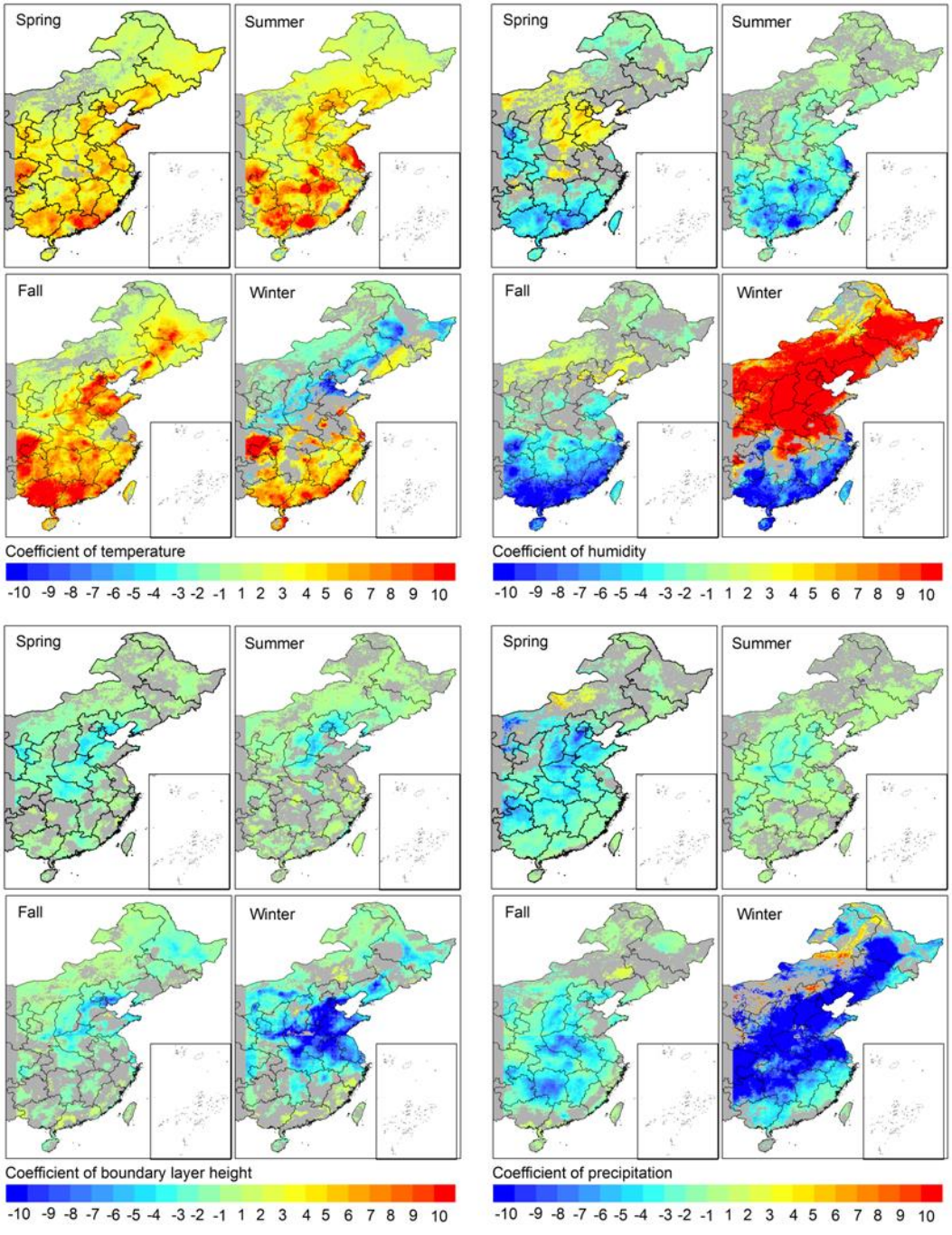

460 **Figure C2: Distribution of the estimated seasonal coefficients of the normalized meteorological parameters in East China.**

https://doi.org/10.5194/acp-2021-28
Preprint. Discussion started: 10 March 2021

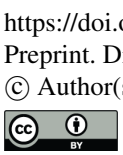

Atmospheric Chemistry and Physics Discussions

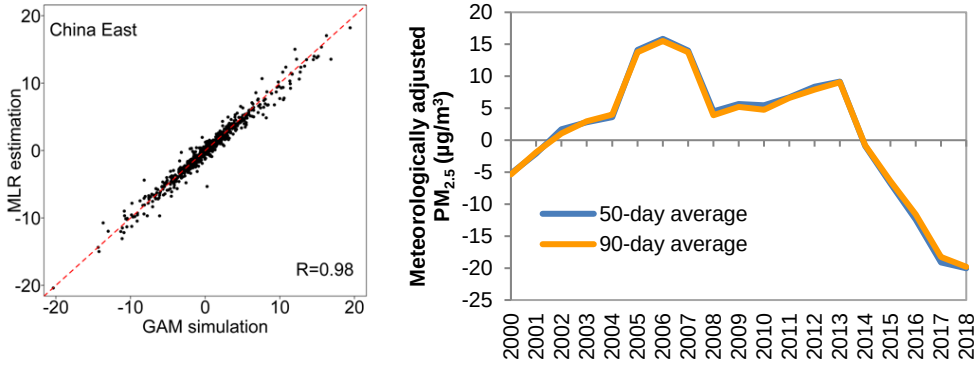

Figure C3: Meteorology-associate $PM_{2.5}$ variations estimated with the MLR and GAM (left), and meteorologically adjusted $PM_{2.5}$ with 50-day seasonal averaging window and 90-day seasonal averaging window (right).

Data availability

All the data used to predict $PM_{2.5}$ concentrations are openly available for download from the websites given in the supplement.

Author contributions

Qingyang Xiao, Guannan Geng, and Qiang Zhang designed the analyses and Qingyang Xiao carried them out. Yixuan Zheng performed the WRF/CMAQ simulations. Xiaomeng Huang optimized the data fusion model. Cuihong Chen, Huizheng Che, Xiaoye Zhang, and Kebin He interpreted the results. Qingyang Xiao and Guannan Geng prepared the manuscript and figures with contributions from all co-authors.

Competing interests

The authors declare that they have no conflict of interest.

Acknowledgments

This work was supported by the National Natural Science Foundation of China (grant no. 42007189, 42005135, 41921005, and 41625020).

https://doi.org/10.5194/acp-2021-28
Preprint. Discussion started: 10 March 2021

Atmospheric Chemistry and Physics Discussions

References

Bian, Y., Huang, Z., Ou, J., Zhong, Z., Xu, Y., Zhang, Z., Xiao, X., Ye, X., Wu, Y., Yin, X., Li, C., Chen, L., Shao, M., and Zheng, J.: Evolution of anthropogenic air pollutant emissions in Guangdong Province, China, from 2006 to 2015, Atmos. Chem. Phys., 19, 11701-11719, 10.5194/acp-19-11701-2019, 2019.

Buchard, V., Randles, C., da Silva, A., Darmenov, A., Colarco, P., Govindaraju, R., Ferrare, R., Hair, J., Beyersdorf, A., and Ziemba, L.: The MERRA-2 aerosol reanalysis, 1980 onward. Part II: Evaluation and case studies, Journal of Climate, 30, 6851-6872, 2017.

Chang, L., Xu, J., Tie, X., and Wu, J.: Impact of the 2015 El Nino event on winter air quality in China, Scientific Reports, 6, 34275, 10.1038/srep34275, 2016.

Chawla, N., Bowyer, K., Hall, L., and Kegelmeyer, W.: SMOTE: Synthetic Minority Over-sampling Technique, J. Artif. Intell. Res. (JAIR), 16, 321-357, 10.1613/jair.953, 2002.

Chawla, N., Lazarevic, A., Hall, L., and Bowyer, K.: SMOTEBoost: Improving Prediction of the Minority Class in Boosting, 107-119 pp., 2003.

Chen, H., Wang, H., Sun, J., Xu, Y., and Yin, Z.: Anthropogenic fine particulate matter pollution will be exacerbated in eastern China due to 21st century GHG warming, Atmos. Chem. Phys., 19, 233-243, 10.5194/acp-19-233-2019, 2019.

Chen, Z., Chen, D., Zhao, C., Kwan, M.-p., Cai, J., Zhuang, Y., Zhao, B., Wang, X., Chen, B., Yang, J., Li, R., He, B., Gao, B., Wang, K., and Xu, B.: Influence of meteorological conditions on PM2.5 concentrations across China: A review of methodology and mechanism, Environment International, 139, 105558, https://doi.org/10.1016/j.envint.2020.105558, 2020.

Cheng, N., Cheng, B., Li, S., and Ning, T.: Effects of meteorology and emission reduction measures on air pollution in Beijing during heating seasons, Atmospheric Pollution Research, 10, 971-979, https://doi.org/10.1016/j.apr.2019.01.005, 2019a.

Cheng, X., Boiyo, R., Zhao, T., Xu, X., Gong, S., Xie, X., and Shang, K.: Climate modulation of Niño3.4 SST-anomalies on air quality change in southern China: Application to seasonal forecast of haze pollution, Atmospheric Research, 225, 157-164, https://doi.org/10.1016/j.atmosres.2019.04.002, 2019b.

Dong, L., Li, S., Yang, J., Shi, W., and Zhang, L.: Investigating the performance of satellite-based models in estimating the surface PM2.5 over China, Chemosphere, 256, 127051, https://doi.org/10.1016/j.chemosphere.2020.127051, 2020.

Feng, J., Liao, H., Li, Y., Zhang, Z., and Tang, Y.: Long-term trends and variations in haze-related weather conditions in north China during 1980–2018 based on emission-weighted stagnation intensity, Atmospheric Environment, 240, 117830, https://doi.org/10.1016/j.atmosenv.2020.117830, 2020.

Geng, G., Xiao, Q., Zheng, Y., Tong, D., Zhang, Y., Zhang, X., Zhang, Q., He, K., and Liu, Y.: Impact of China's Air Pollution Prevention and Control Action Plan on PM2.5 chemical composition over eastern China, Science China Earth Sciences, 62, 1872-1884, 10.1007/s11430-018-9353-x, 2019.

Ghorbani, R., and Ghousi, R.: Comparing Different Resampling Methods in Predicting Students' Performance Using Machine Learning Techniques, IEEE Access, 8, 67899-67911, 10.1109/ACCESS.2020.2986809, 2020.

Gong, P., Li, X., and Zhang, W.: 40-Year (1978–2017) human settlement changes in China reflected by impervious surfaces from satellite remote sensing, Science Bulletin, 64, 756-763, https://doi.org/10.1016/j.scib.2019.04.024, 2019a.

Gong, P., Liu, H., Zhang, M., Li, C., Wang, J., Huang, H., Clinton, N., Ji, L., Li, W., Bai, Y., Chen, B., Xu, B., Zhu, Z., Yuan, C., Ping Suen, H., Guo, J., Xu, N., Li, W., Zhao, Y., Yang, J., Yu, C., Wang, X., Fu, H., Yu, L., Dronova, I., Hui, F., Cheng, X., Shi, X., Xiao, F., Liu, Q., and Song, L.: Stable classification with limited sample: transferring a 30-m resolution sample set collected in 2015 to mapping 10-m resolution global land cover in 2017, Science Bulletin, 64, 370-373, https://doi.org/10.1016/j.scib.2019.03.002, 2019b.

Grange, S. K., Carslaw, D. C., Lewis, A. C., Boleti, E., and Hueglin, C.: Random forest meteorological normalisation models for Swiss PM10 trend analysis, Atmos. Chem. Phys., 18, 6223-6239, 10.5194/acp-18-6223-2018, 2018.

Guan, D., Su, X., Zhang, Q., Peters, G. P., Liu, Z., Lei, Y., and He, K.: The socioeconomic drivers of China's primary PM2. 5 emissions, Environmental Research Letters, 9, 024010, 2014.

He, C., Liu, R., Wang, X., Liu, S. C., Zhou, T., and Liao, W.: How does El Niño-Southern Oscillation modulate the interannual variability of winter haze days over eastern China?, Science of The Total Environment, 651, 1892-1902, https://doi.org/10.1016/j.scitotenv.2018.10.100, 2019.

He, J., Gong, S., Yu, Y., Yu, L., Wu, L., Mao, H., Song, C., Zhao, S., Liu, H., Li, X., and Li, R.: Air pollution characteristics and their relation to meteorological conditions during 2014–2015 in major Chinese cities, Environmental Pollution, 223, 484-496, https://doi.org/10.1016/j.envpol.2017.01.050, 2017.

He, L., and Wang, D.: Pollution characteristics and influencing factors of PM2.5 in Fuxin City, Ecol. Sci., 1, 201-208, 2017.

He, Q., and Huang, B.: Satellite-based mapping of daily high-resolution ground PM 2.5 in China via space-time regression modeling, Remote Sensing of Environment, 206, 72-83, 2018.

Hsu, N., Jeong, M. J., Bettenhausen, C., Sayer, A., Hansell, R., Seftor, C., Huang, J., and Tsay, S. C.: Enhanced Deep Blue aerosol retrieval algorithm: The second generation, Journal of Geophysical Research: Atmospheres, 118, 9296-9315, 2013.

Jeong, J. I., and Park, R. J.: Winter monsoon variability and its impact on aerosol concentrations in East Asia, Environmental Pollution, 221, 285-292, https://doi.org/10.1016/j.envpol.2016.11.075, 2017.

https://doi.org/10.5194/acp-2021-28
Preprint. Discussion started: 10 March 2021

Atmospheric Chemistry and Physics Discussions

Jinnagara Puttaswamy, S., Nguyen, H. M., Braverman, A., Hu, X., and Liu, Y.: Statistical data fusion of multi-sensor AOD over the Continental United States, Geocarto International, 29, 48-64, 2014.

Levy, R., Mattoo, S., Munchak, L., Remer, L., Sayer, A., Patadia, F., and Hsu, N.: The Collection 6 MODIS aerosol products over land and ocean, Atmospheric Measurement Techniques, 6, 2989-3034, 2013.

Li, M., Liu, H., Geng, G. N., Hong, C. P., Liu, F., Song, Y., Tong, D., Zheng, B., Cui, H. Y., Man, H. Y., Zhang, Q., and He, K. B.: Anthropogenic emission inventories in China: a review, Natl. Sci. Rev., 4, 834-866, 10.1093/nsr/nwx150, 2017a.

Li, M., Zhang, Q., Kurokawa, J. I., Woo, J. H., He, K., Lu, Z., Ohara, T., Song, Y., Streets, D. G., Carmichael, G. R., Cheng, Y., Hong, C., Huo, H., Jiang, X., Kang, S., Liu, F., Su, H., and Zheng, B.: MIX: a mosaic Asian anthropogenic emission inventory under the international collaboration framework of the MICS-Asia and HTAP, Atmos. Chem. Phys., 17, 935-963, 10.5194/acp-17-935-2017, 2017b.

Liu, F., Zhang, Q., Tong, D., Zheng, B., Li, M., Huo, H., and He, K. B.: High-resolution inventory of technologies, activities, and emissions of coal-fired power plants in China from 1990 to 2010, Atmos. Chem. Phys., 15, 13299-13317, 10.5194/acp-15-13299-2015, 2015.

Liu, R., Liao, H., and Chang, W.: Impact of climate change on aerosol concentrations in eastern China based on Atmospheric Chemistry and Climate Model Intercomparison Project (ACCMIP) datasets, Chin J Atmos Sci, 41, 739-751, 2017a.

Liu, T. T., Gong, S. L., He, J. J., Yu, M., Wang, Q. F., Li, H. R., Liu, W., Zhang, J., Li, L., Wang, X. G., Li, S. L., Lu, Y. L., Du, H. T., Wang, Y. Q., Zhou, C. H., Liu, H. L., and Zhao, Q. C.: Attributions of meteorological and emission factors to the 2015 winter severe haze pollution episodes in China's Jing-Jin-Ji area, Atmospheric Chemistry and Physics, 17, 2971-2980, 10.5194/acp-17-2971-2017, 2017b.

Liu, Y., Paciorek, C. J., and Koutrakis, P.: Estimating regional spatial and temporal variability of PM2. 5 concentrations using satellite data, meteorology, and land use information, Environmental health perspectives, 117, 886, 2009.

Ma, Z., Liu, R., Liu, Y., and Bi, J.: Effects of air pollution control policies on PM2.5 pollution improvement in China from 2005 to 2017: a satellite-based perspective, Atmos. Chem. Phys., 19, 6861-6877, 10.5194/acp-19-6861-2019, 2019.

Maji, K. J., Ye, W.-F., Arora, M., and Nagendra, S. M. S.: Ozone pollution in Chinese cities: Assessment of seasonal variation, health effects and economic burden, Environmental Pollution, 247, 792-801, https://doi.org/10.1016/j.envpol.2019.01.049, 2019.

NCEP: NCEP FNL Operational Model Global Tropospheric Analyses, continuing from July 1999, https://doi.org/10.5065/D6M043C6, 2000.

Pearce, J. L., Beringer, J., Nicholls, N., Hyndman, R. J., and Tapper, N. J.: Quantifying the influence of local meteorology on air quality using generalized additive models, Atmospheric Environment, 45, 1328-1336, https://doi.org/10.1016/j.atmosenv.2010.11.051, 2011.

Qiu, D., Liu, J., Zhu, L., Mo, L., and Zhang, Z.: Particulate matter assessment of a wetland in Beijing, Journal of Environmental Sciences, 36, 93-101, https://doi.org/10.1016/j.jes.2015.04.016, 2015.

Qu, L., Liu, S., Ma, L., Zhang, Z., Du, J., Zhou, Y., and Meng, F.: Evaluating the meteorological normalized PM2.5 trend (2014–2019) in the "2+26" region of China using an ensemble learning technique, Environmental Pollution, 266, 115346, https://doi.org/10.1016/j.envpol.2020.115346, 2020.

Randles, C., da Silva, A. M., Buchard, V., Colarco, P., Darmenov, A., Govindaraju, R., Smirnov, A., Holben, B., Ferrare, R., and Hair, J.: The MERRA-2 aerosol reanalysis, 1980 onward. Part I: System description and data assimilation evaluation, Journal of Climate, 30, 6823-6850, 2017.

Ruijin, L., Hong, L., Wenyuan, C., Tianhang, Z., Shaofei, J., and Technology: Impact of Climate Change on Aerosol Concentrations in Eastern China Based on Atmospheric Chemistry and Climate Model Intercomparison Project (ACCMIP) Datasets, Chinese Journal of Atmospheric ences, 2017.

Sá, E., Tchepel, O., Carvalho, A., and Borrego, C.: Meteorological driven changes on air quality over Portugal: a KZ filter application, Atmospheric Pollution Research, 6, 979-989, https://doi.org/10.1016/j.apr.2015.05.003, 2015.

Saputra, A., and Suharjito: Fraud Detection using Machine Learning in e-Commerce, Int. J. Adv. Comput. Sci. Appl., 10, 332-339, 2019.

Shen, H., Tao, S., Chen, Y., Ciais, P., Güneralp, B., Ru, M., Zhong, Q., Yun, X., Zhu, X., Huang, T., Tao, W., Chen, Y., Li, B., Wang, X., Liu, W., Liu, J., and Zhao, S.: Urbanization-induced population migration has reduced ambient PM(2.5) concentrations in China, Science advances, 3, e1700300-e1700300, 10.1126/sciadv.1700300, 2017.

Torgo, L.: Data Mining with R: Learning with Case Studies, Chapman & Hall/CRC, 2010.

Vu, T. V., Shi, Z., Cheng, J., Zhang, Q., He, K., Wang, S., and Harrison, R. M.: Assessing the impact of clean air action on air quality trends in Beijing using a machine learning technique, Atmos. Chem. Phys., 19, 11303-11314, 10.5194/acp-19-11303-2019, 2019.

Wang, H. J., and Chen, H. P.: Understanding the recent trend of haze pollution in eastern China: roles of climate change, Atmos. Chem. Phys., 16, 4205-4211, 10.5194/acp-16-4205-2016, 2016.

Wang, P., Guo, H., Hu, J., Kota, S. H., Ying, Q., and Zhang, H.: Responses of PM2.5 and O3 concentrations to changes of meteorology and emissions in China, Science of The Total Environment, 662, 297-306, https://doi.org/10.1016/j.scitotenv.2019.01.227, 2019a.

Wang, X., and Zhang, R.: Effects of atmospheric circulations on the interannual variation in PM2.5 concentrations over the Beijing–Tianjin–Hebei region in 2013–2018, Atmos. Chem. Phys., 20, 7667-7682, 10.5194/acp-20-7667-2020, 2020.

Wang, Y., Yuan, Q., Li, T., Shen, H., Zheng, L., and Zhang, L.: Evaluation and comparison of MODIS Collection 6.1 aerosol optical depth against AERONET over regions in China with multifarious underlying surfaces, Atmospheric Environment, 200, 280-301, https://doi.org/10.1016/j.atmosenv.2018.12.023, 2019b.

Wei, J., Li, Z., Cribb, M., Huang, W., Xue, W., Sun, L., Guo, J., Peng, Y., Li, J., Lyapustin, A., Liu, L., Wu, H., and Song, Y.: Improved 1 km resolution PM2.5 estimates across China using enhanced space–time extremely randomized trees, Atmos. Chem. Phys., 20, 3273-3289, 10.5194/acp-20-3273-2020, 2020.

Xiao, Q., Chang, H. H., Geng, G., and Liu, Y.: An Ensemble Machine-Learning Model To Predict Historical PM2.5 Concentrations in China from Satellite Data, Environmental Science & Technology, 52, 13260-13269, 10.1021/acs.est.8b02917, 2018.

Xiao, Q., Liang, F., Ning, M., Zhang, Q., Bi, J., He, K., Lei, Y., and Liu, Y.: High-resolution maps on long-term PM2.5 exposure and associated health burden in China: 2000-2018, Drafting, 2020.

Xiao, Q., Geng, G., Cheng, J., Liang, F., Li, R., Meng, X., Xue, T., Huang, X., Kan, H., Zhang, Q., and He, K.: Evaluation of gap-filling approaches in satellite-based daily PM2.5 prediction models, Atmospheric Environment, 244, 117921, https://doi.org/10.1016/j.atmosenv.2020.117921, 2021a.

Xiao, Q., Liang, F., Ning, M., Zhang, Q., Bi, J., He, K., Lei, Y., and Liu, Y.: The long-term trend of PM2.5-related mortality in China: The effects of source data selection, Chemosphere, 263, 127894, https://doi.org/10.1016/j.chemosphere.2020.127894, 2021b.

Xu, Y., Xue, W., Lei, Y., Huang, Q., Zhao, Y., Cheng, S., Ren, Z., and Wang, J.: Spatiotemporal variation in the impact of meteorological conditions on PM2.5 pollution in China from 2000 to 2017, Atmospheric Environment, 223, 117215, https://doi.org/10.1016/j.atmosenv.2019.117215, 2020.

Xue, T., Zheng, Y., Tong, D., Zheng, B., Li, X., Zhu, T., and Zhang, Q.: Spatiotemporal continuous estimates of PM2.5 concentrations in China, 2000–2016: A machine learning method with inputs from satellites, chemical transport model, and ground observations, Environment International, 123, 345-357, https://doi.org/10.1016/j.envint.2018.11.075, 2019.

Yanosky, J. D., Paciorek, C. J., Laden, F., Hart, J. E., Puett, R. C., Liao, D., and Suh, H. H.: Spatio-temporal modeling of particulate air pollution in the conterminous United States using geographic and meteorological predictors, Environmental Health, 13, 63, 2014.

Yi, K., Liu, J., Wang, X., Ma, J., Hu, J., Wan, Y., Xu, J., Yang, H., Liu, H., Xiang, S., and Tao, S.: A combined Arctic-tropical climate pattern controlling the inter-annual climate variability of wintertime PM2.5 over the North China Plain, Environmental Pollution, 245, 607-615, https://doi.org/10.1016/j.envpol.2018.10.136, 2019.

Yin, Z., Wang, H., and Yuan, D.: Interdecadal increase of haze in winter over North China and the Huang-huai Area and the weakening of the East Asia Winter Monsoon, Kexue Tongbao/Chinese Science Bulletin, 60, 1395-1400, 10.1360/N972014-01348, 2015.

Yin, Z., and Wang, H.: The relationship between the subtropical Western Pacific SST and haze over North-Central North China Plain, International Journal of Climatology, 36, 3479-3491, 10.1002/joc.4570, 2016.

Yin, Z., and Wang, H.: Role of atmospheric circulations in haze pollution in December 2016, Atmospheric Chemistry and Physics, 17, 11673-11681, 10.5194/acp-17-11673-2017, 2017.

Yin, Z., Wang, H., and Chen, H.: Understanding severe winter haze events in the North China Plain in 2014: Roles of climate anomalies, Atmospheric Chemistry and Physics, 17, 1641-1651, 10.5194/acp-17-1641-2017, 2017.

Yin, Z., and Wang, H.: The strengthening relationship between Eurasian snow cover and December haze days in central North China after the mid-1990s, Atmospheric Chemistry and Physics, 18, 4753-4763, 10.5194/acp-18-4753-2018, 2018.

Zhai, S., Jacob, D. J., Wang, X., Shen, L., Li, K., Zhang, Y., Gui, K., Zhao, T., and Liao, H.: Fine particulate matter (PM2.5) trends in China, 2013–2018: separating contributions from anthropogenic emissions and meteorology, Atmos. Chem. Phys., 19, 11031-11041, 10.5194/acp-19-11031-2019, 2019.

Zhang, L., Wang, T., Lv, M. Y., and Zhang, Q.: On the severe haze in Beijing during January 2013: Unraveling the effects of meteorological anomalies with WRF-Chem, Atmospheric Environment, 104, 11-21, 10.1016/j.atmosenv.2015.01.001, 2015.

Zhang, Q., Zheng, Y., Tong, D., Shao, M., Wang, S., Zhang, Y., Xu, X., Wang, J., He, H., Liu, W., Ding, Y., Lei, Y., Li, J., Wang, Z., Zhang, X., Wang, Y., Cheng, J., Liu, Y., Shi, Q., Yan, L., Geng, G., Hong, C., Li, M., Liu, F., Zheng, B., Cao, J., Ding, A., Gao, J., Fu, Q., Huo, J., Liu, B., Liu, Z., Yang, F., He, K., and Hao, J.: Drivers of improved PM2.5 air quality in China from 2013 to 2017, Proceedings of the National Academy of Sciences, 116, 24463, 10.1073/pnas.1907956116, 2019a.

Zhang, X., Zhong, J., Wang, J., Wang, Y., and Liu, Y.: The interdecadal worsening of weather conditions affecting aerosol pollution in the Beijing area in relation to climate warming, Atmos. Chem. Phys., 18, 5991-5999, 10.5194/acp-18-5991-2018, 2018.

Zhang, X., Xu, X., Ding, Y., Liu, Y., Zhang, H., Wang, Y., and Zhong, J.: The impact of meteorological changes from 2013 to 2017 on PM2.5 mass reduction in key regions in China, Science China Earth Sciences, 62, 1885-1902, 10.1007/s11430-019-9343-3, 2019b.

Zhang, Y., Vu, T. V., Sun, J., He, J., Shen, X., Lin, W., Zhang, X., Zhong, J., Gao, W., Wang, Y., Fu, T. M., Ma, Y., Li, W., and Shi, Z.: Significant Changes in Chemistry of Fine Particles in Wintertime Beijing from 2007 to 2017: Impact of Clean Air Actions, Environmental Science & Technology, 54, 1344-1352, 10.1021/acs.est.9b04678, 2020.

Zhao, X., Zhao, P., Xu, J., Meng, W., Pu, W., Dong, F., He, D., and Shi, Q.: Analysis of a winter regional haze event and its formation mechanism in the North China Plain, Atmospheric Chemistry and Physics, 13, 5685-5696, 2013.

Zheng, B., Tong, D., Li, M., Liu, F., Hong, C., Geng, G., Li, H., Li, X., Peng, L., Qi, J., Yan, L., Zhang, Y., Zhao, H., Zheng, Y., He, K., and Zhang, Q.: Trends in China's anthropogenic emissions since 2010 as the consequence of clean air actions, Atmos. Chem. Phys., 18, 14095-14111, 10.5194/acp-18-14095-2018, 2018.

Zheng, Y. X., Xue, T., Zhang, Q., Geng, G. N., Tong, D., Li, X., and He, K. B.: Air quality improvements and health benefits from China's clean air action since 2013, Environmental Research Letters, 12, ARTN 114020

https://doi.org/10.5194/acp-2021-28
Preprint. Discussion started: 10 March 2021

Atmospheric Chemistry and Physics Discussions

10.1088/1748-9326/aa8a32, 2017.
Zhu, J., Liao, H., and Li, J.: Increases in aerosol concentrations over eastern China due to the decadal-scale weakening of the East Asian summer monsoon, Geophysical Research Letters, 39, 10.1029/2012GL051428, 2012.

645

https://doi.org/10.5194/acp-2021-28
Preprint. Discussion started: 10 March 2021

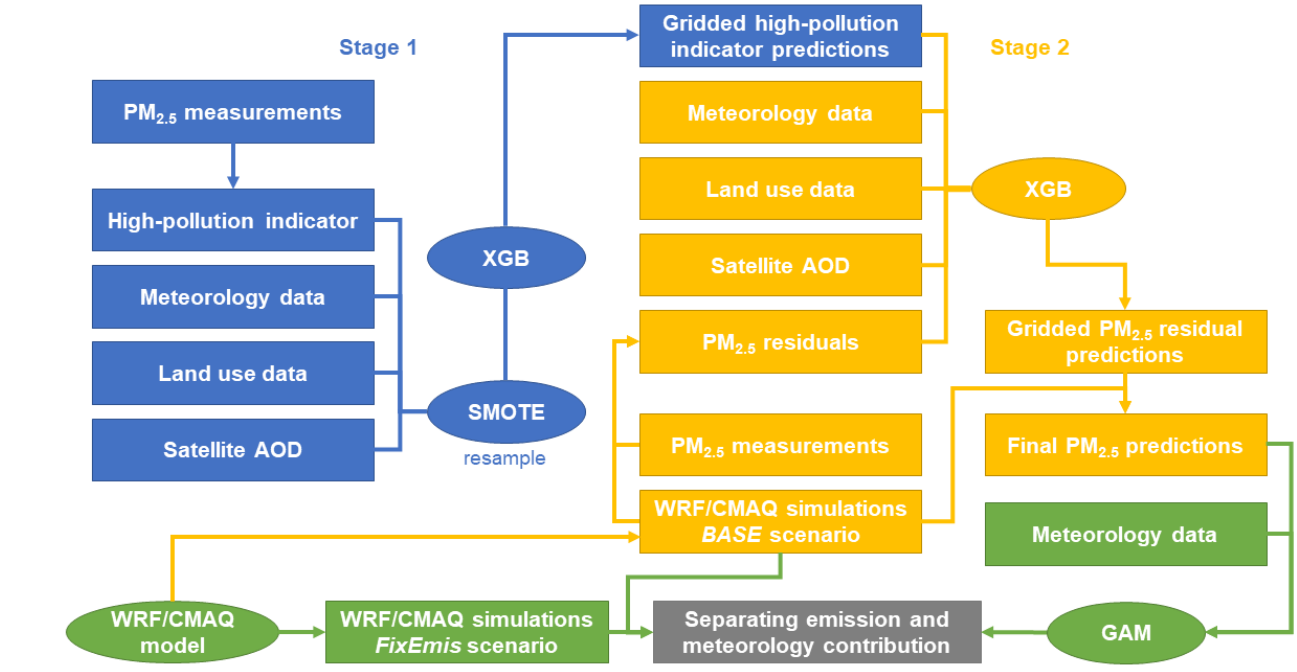

Figure 1: Methodology framework of this study.

https://doi.org/10.5194/acp-2021-28
Preprint. Discussion started: 10 March 2021

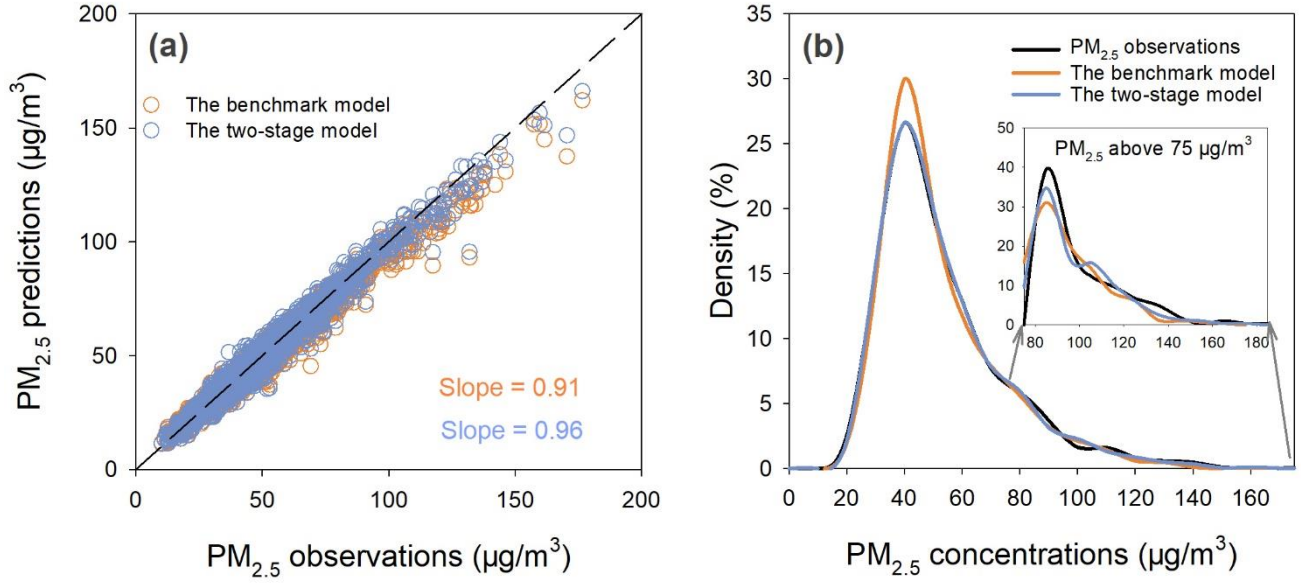

650 **Figure 2: Comparisons between the two-stage model and the benchmark model. (a) The scatter plot of the two-stage model predictions and the benchmark model predictions against ground observations in the five-fold cross-validation (CV). (b) Density distributions of the two-stage model predictions, the benchmark model predictions and the $PM_{2.5}$ observations in the five-fold CV.**

https://doi.org/10.5194/acp-2021-28
Preprint. Discussion started: 10 March 2021

Atmospheric Chemistry and Physics Discussions

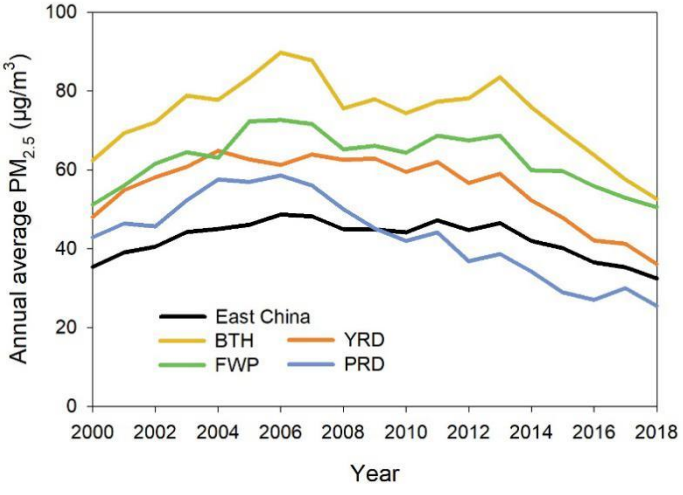

Figure 3: Temporal trends of the annual average satellite-based $PM_{2.5}$ concentrations over East China and the key regions during 2000–2018. BTH: Beijing-Tianjin-Hebei; FWP: Fen-wei Plain; YRD: Yangtze River Delta; PRD: Pearl River Delta.

655

https://doi.org/10.5194/acp-2021-28
Preprint. Discussion started: 10 March 2021

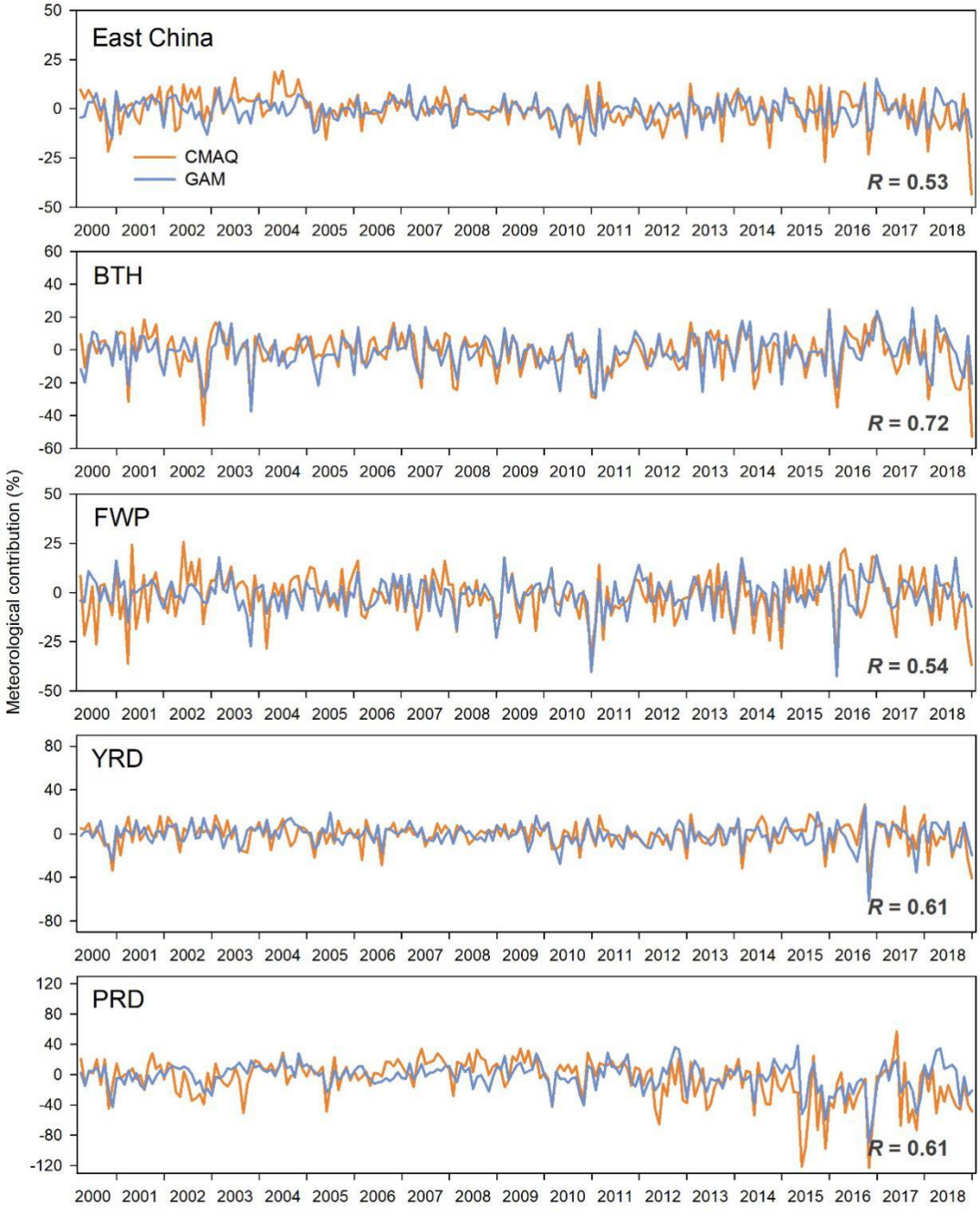

Figure 4: Fractional contribution of meteorology to $PM_{2.5}$ concentrations on the monthly scale during 2000–2018, estimated from CMAQ (the orange line) and GAM (the blue line).

https://doi.org/10.5194/acp-2021-28
Preprint. Discussion started: 10 March 2021

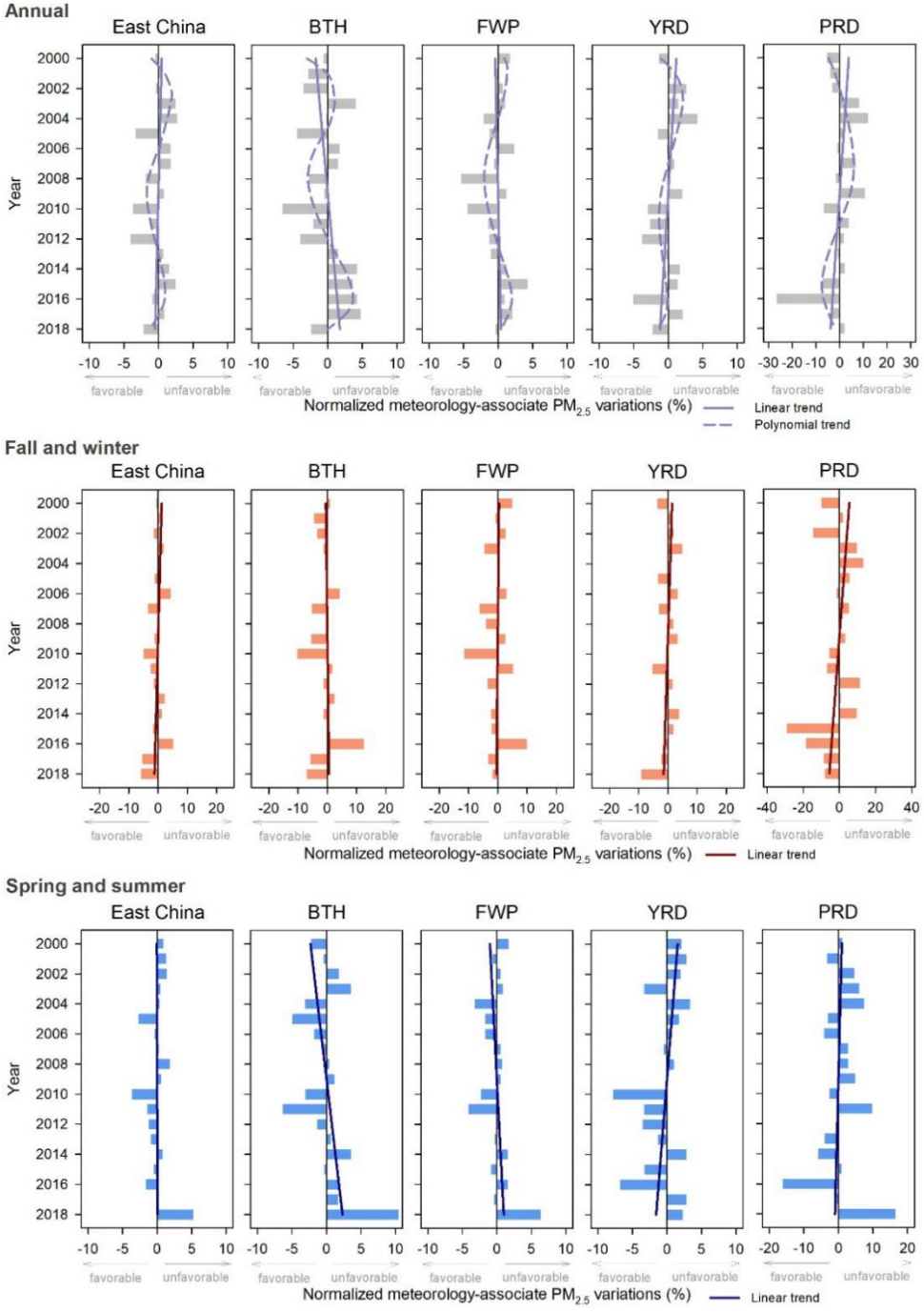

Figure 5: The GAM estimated relative impact of meteorology on annual average $PM_{2.5}$ (top row), relative impact of meteorology on average $PM_{2.5}$ in fall-winter (September, October, November, December, January in next year, and February in next year) (middle), and relative impact of meteorology on average $PM_{2.5}$ in spring-summer (bottom row) with the long-term trends estimated by polynomial and linear regression over East China, BTH, FWP, YRD, and PRD.

https://doi.org/10.5194/acp-2021-28
Preprint. Discussion started: 10 March 2021

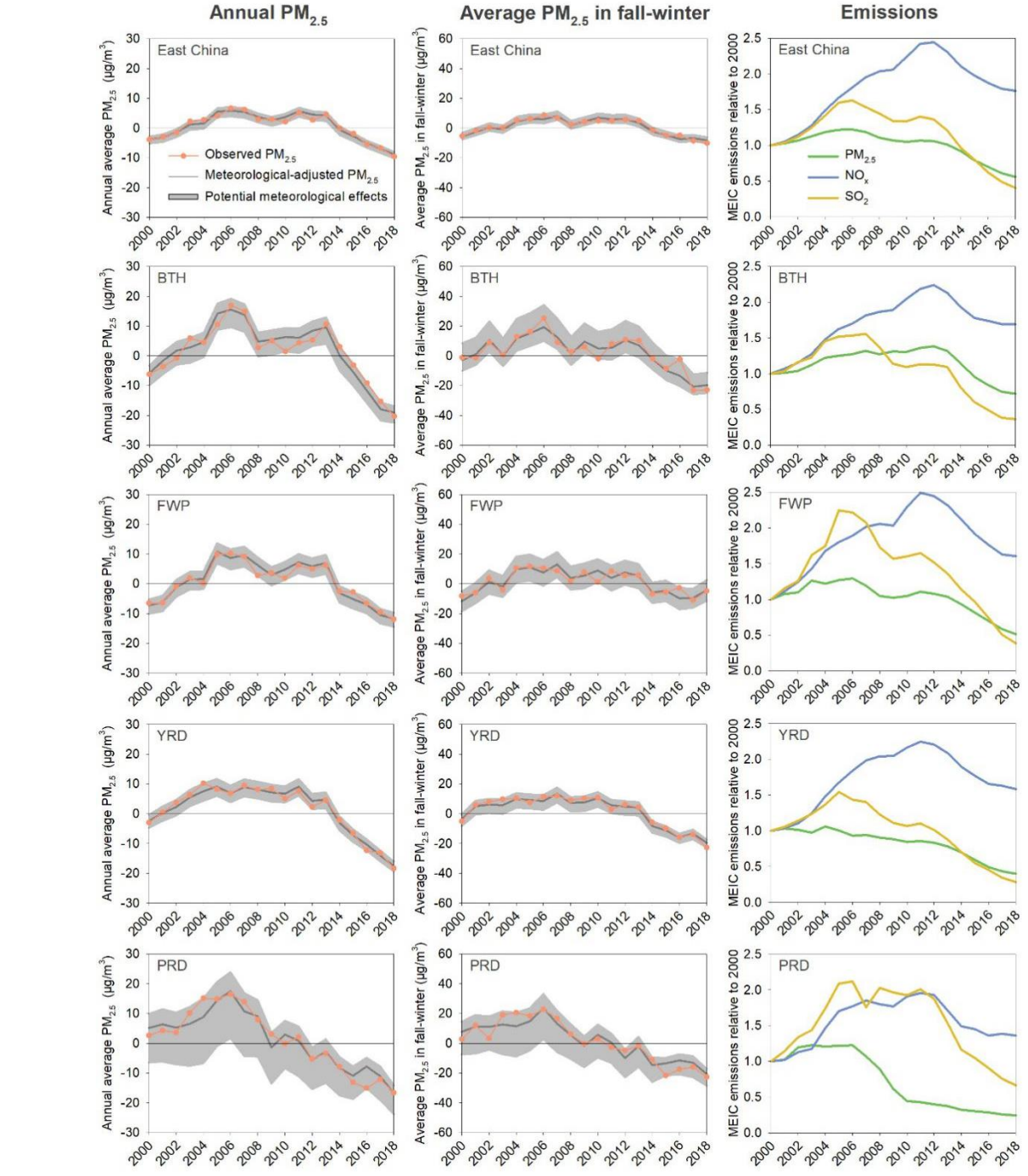

Figure 6: Time series of the annual average (left column) and fall-winter average (middle column) $PM_{2.5}$ concentrations before (the orange line) and after (the gray line) the adjustment of the meteorological effects from 2000–2018 using GAM. The gray shadow shows the potential range of the observed $PM_{2.5}$ due to meteorological effects. The right column shows the MEIC emissions of $PM_{2.5}$, NO_x, and SO_2, respectively.

https://doi.org/10.5194/acp-2021-28
Preprint. Discussion started: 10 March 2021

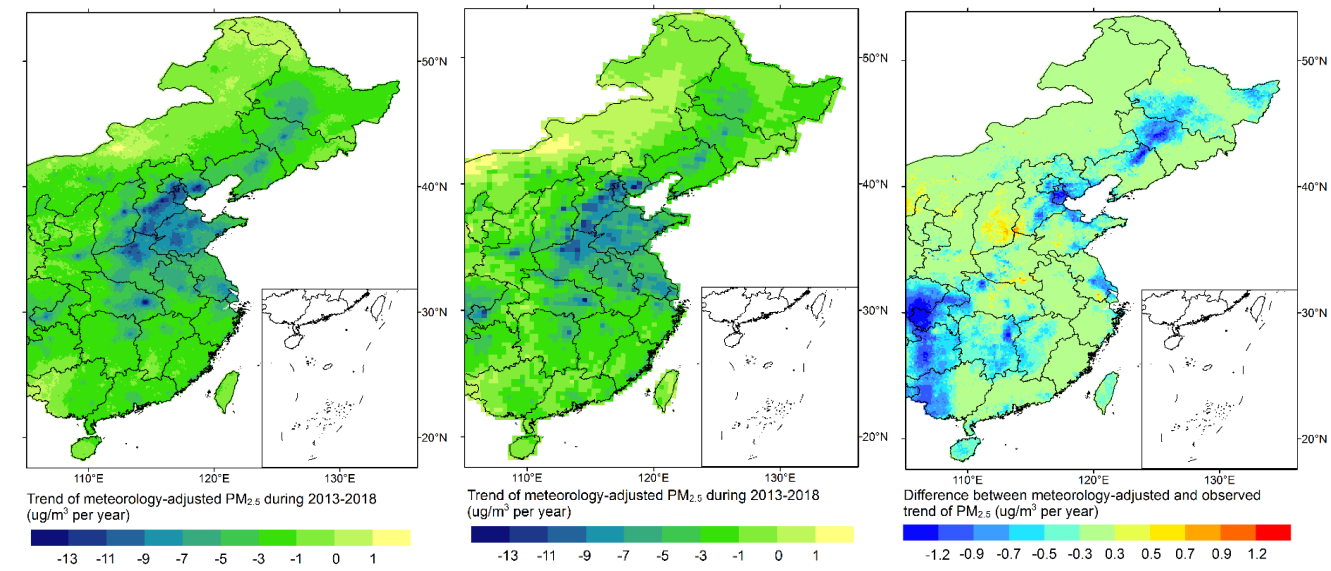

Figure 7: Left: Spatial distribution of the $PM_{2.5}$ decrease rate during 2013–2018 after adjusting for the meteorological effects using GAM. Middle: Spatial distribution of the $PM_{2.5}$ decrease rate during 2013–2018 after adjusting for the meteorological effects using CMAQ. Right: The difference in the $PM_{2.5}$ decrease rate before and after the adjustment for the meteorological effects using GAM.